REPORT DOCUMENTATION PAGE

Form Approved
OMB No. 0704-0188

1. AGENCY USE ONLY (*Leave Blank*)	2. REPORT DATE	3. REPORT TYPE AND DATES COVERED
	5Jan98	Final Report 2Jul97 - 2Jan98

4. TITLE AND SUBTITLE
Frequency-Agile High-Power-Density Transducers:
Draft/Final Technical Report

5. FUNDING NUMBERS
C N00014-97-C-0298

6. AUTHOR(S)
Keith Bridger, John M. Sewell, Philip M. Kuhn,
Edward J. Passaro, Yong S. Cho, Herbert Giesche,
Steven M. Pilgrim, and Vasantha R.W. Amarakoon

7. PERFORMING ORGANIZATION NAME(S) AND ADDRESS(ES)
Active Signal Technologies, Incorporated
13025 Beaver Dam Road
Cockeysville, MD 21030, AND

New York State College of Ceramics at Alfred University
Alfred, NY 14802

8. PERFORMING ORGANIZATION REPORT NUMBER

9. SPONSORING/MONITORING AGENCY NAME(S) AND ADDRESS(ES)
Office of Naval Research
800 North Quincy Street
Arlington, VA 22217-5660

10. SPONSORING/MONITORING AGENCY REPORT NUMBER

11. SUPPLEMENTARY NOTES

12a. DISTRIBUTION/AVAILABILITY STATEMENT
Approved for public release; distribution unlimited.

12b. DISTRIBUTION CODE

13. ABSTRACT (*Maximum 200 words*)

Report developed under STTR contract.
This report documents a design study aimed at producing broader bandwidth, high-power transducers for Navy applications in littoral waters. The top-to-bottom study included both ceramic driver processing and the transducer design itself. Active Signal Technologies and Alfred University investigated a novel processing method involving coating the ceramic particles prior to densification and it substantially increased the room-temperature electrically-induced strains available from the ceramic without significantly increasing dielectric loss. This strain increase could translate to a >3-dB increase in power density for the broadband transducers. Active Signal investigated a range of transducer classes including Class IV and VII Flextensional, Tonpilz, Moment Bender, Flexural Disk, and Split Cylinder. Substituting graphite-epoxy for aluminum in the radiating surface produced ~30% increases in bandwidth in most of the classes. With this and other parametric adjustments, designs that met feasibility criteria (power, efficiency, depth dependence, etc.) but had fractional bandwidths >80% were prepared. The recommended design was a graphite-epoxy Class-IV Flextensional.

14. SUBJECT TERMS	15. NUMBER OF PAGES
Broadband transducer design, lead magnesium niobate, transducer, STTR Report	42
	16. PRICE CODE

17. SECURITY CLASSIFICATION OF REPORT	18. SECURITY CLASSIFICATION OF THIS PAGE	19. SECURITY CLASSIFICATION OF ABSTRACT	20. LIMITATION OF ABSTRACT
Unclassified	Unclassified	Unclassified	UL

REF D

PHASE-I FINAL REPORT

CONTRACT NUMBER N00014 - 97 - C - 0298

FREQUENCY-AGILE HIGH-POWER-DENSITY TRANSDUCERS

Draft/Final Technical Report
CLIN 0001AD
July 02, 1997 - January 02, 1998

Submitted by:

Active Signal Technologies, Inc.
13025 Beaver Dam Rd
Cockeysville, MD 21030
Phone: 410 433-1572

Keith Bridger, John M. Sewell, Philip Kuhn, and Edward J. Passaro

and

New York State College of Ceramics at Alfred University
Alfred, NY 14802

Yong S. Cho, Herbert Giesche, Steven M. Pilgrim
and Vasantha R. W. Amarakoon

Principal Investigator:

Keith Bridger

Submitted on:

January 05, 1998

Submitted to:

Program Officer
Office of Naval Research
800 North Quincy Street
Arlington, VA 22217-5660

Administrative Contracting Officer
DCMC Baltimore
Attention: Code S2101A
200 Towsontown Boulevard, West
Towson, MD 21204-5299

1. BACKGROUND

Shallow water Anti-Submarine Warfare (ASW) and Mine Warfare (MIW) sonar systems require broadband transducer arrays to deliver the special waveforms that can resolve features in the presence of high reverberation levels and multipath effects. Whereas broadband waveforms and the signal processing required to interpret them have been well-developed in radar technology the lack of suitable lightweight broadband projectors has inhibited more widespread use of the technology in ASW/MIW. The problem can be described semi quantitatively in terms of a transducer figure of merit (FOM) developed by workers at the Naval Undersea Warfare Center (NUWC):

$$FOM = \frac{P\Delta f}{mf_0^2}$$

where P is the acoustic power output (W), m the mass of the projector (kg), and f_0 and Δf the center frequency and -3 dB bandwidth (kHz), respectively. Current projectors have FOM values ~30 W/kg/kHz which limits their use in high-bandwidth applications because the projector weights become excessively large (~50 ton).

Recent breakthrough developments by Lockheed Martin, particularly in the area of novel materials with enormous increases in power density have enabled transducers with FOM ~200 W/kg/kHz to be fabricated using electrostrictive lead magnesium niobate (PMN) drivers. This high FOM can make the use of broadband waveforms practical with a high power, relatively lightweight projector. This program seeks to enhance the opportunity for near-term practical implementation of this technology by addressing the key shortfalls in processing and electrical properties that are currently impeding widespread adoption of PMN. Our two-pronged approach comprises both fine tuning the physical properties and electrical characteristics of this material in addition to the development of alternative transducer designs which optimize bandwidth rather than power. PMN as a practical option for field service, as opposed to research investigation, is a relative newcomer to the Navy sonar materials arsenal, compared to conventional ceramic lead zirconate titanate (PZT) which has had the benefit of over 40 years of dedicated materials science and product development effort. The first PMN transducer was built in 1990.

While extensive testing of electrostrictive materials based on PMN has clearly demonstrated its superior sound pressure level compared to conventional piezoelectrics, there are important power conditioning issues that must be addressed when utilizing transducers built from PMN. In order to support the extremely compact and lightweight transducer designs that are enabled by PMN, much more attention must be paid to the power delivery infrastructure, which, in practical terms, translates into cable diameters, and size and number of power amplifiers.

In order to bring the specifications for the power conditioning system into a practically realizable envelope, it will be necessary to carefully tailor the material processing and properties to overcome the following challenges: sensitivity to contaminants and processing variables arising in the synthesis of large batches, a limited value of electromechanical coupling, and some lower than conventional mechanical properties. The sensitivity of this high-performance material can be evidenced by the fact that only Lockheed Martin has been able to produce material in large quantities with the correct high-strain properties, and even some of their batches have been reported to have flaws resulting for instance in some low strength values. The relatively low coupling coefficients are currently common to all these materials. An underlying hypothesis of the present STTR program is that these limitations are often accompanied by changes in the presence

and distribution of grain boundary phases. We believe that proper control of the formation and distribution of grain boundary phases will not only ameliorate the limitations arising from batch-to-batch variations but will also boost the coupling coefficients of the materials.

The transducer of choice for ASW systems has been selected from either tonpilz or flextensional classes mostly based on power density considerations. These transducers are, however, not necessarily optimized for bandwidth. Typical designs currently have ~33% relative bandwidth ($Q_m = 3$) which implies that a tactical array operating over a wide bandwidth (e.g., 1 - 6 kHz) requires at least 3 transducer types (or subarrays) with center frequencies evenly distributed across that band. In the present program, Active Signal Technologies, Inc. (Active Signal) has critically examined a variety of transducer classes using both aluminum (Al) and graphite-epoxy (GrEp) radiators to produce designs that can cover the 1-6 kHz band with just 2 transducers.

While PMN can reduce the size of a high-power array and its towbody by up to a factor of ten, it requires application of an external dc bias voltage which leads to very high voltages (>5 kV) on the tow cable which in turn makes the size of that cable and its winch significant in terms of ship impact. The cable alone can weigh much more than the towbody and transducer array combined. Using electronic designs developed in this program, we believe we can significantly reduce this cable voltage from 6.8 kV to just 2.8 kV (a similar voltage to that demanded by a corresponding PZT system), and hence significantly diminish ship impact of a system using PMN transducers.

In summary, Active Signal is developing a transducer for high bandwidth that, when coupled with the material developed at the New York State College of Ceramics at Alfred University (Alfred), will enable projection of the waveforms required to resolve targets in shallow water. Active Signal regards this development not only as a resolution to this critical Navy challenge but also as an opportunity for insertion into its evolving non-invasive intracranial pressure (ICP) medical sensor. This acoustic device uses sensors similar in size to the higher frequency transducers used in MIW and so we foresee valuable commercial spin-off from this program.

2. PHASE 1 TECHNICAL OBJECTIVES

The overall goal of this Phase 1 program, as proposed, was to design and test a novel broadband transducer having FOM > 200 W/kg/kHz and a fractional bandwidth > 50%. Achieving this required meeting technical objectives in both materials development and transducer design. These objectives are listed below:

1) Produce an electrostrictive material with high coupling coefficient ($k > 0.6$)
   - address the addition of controlled amounts of selected cations to pre-calcined base composition of PMN
   - assess the utility of grain boundary and core shell structures for controlled property modification of electrostrictive materials, specifically as applied to electromechanical coupling and impedance response.

2) Develop a broad bandwidth transducer design with high FOM
   - develop a list of viable design options
   - sketch and model the performance (SL vs *f*) of each design
   - assess the predicted performance of each design using one set of material properties making comparison with a class-IV flextensional
   - assess the optimum performance achievable using material properties supplied by Alfred and prioritize the material property development

In addition to the objectives from our initially submitted proposal, listed above, Active Signal also recognized the system implications of the bias voltage requirement and undertook the challenge of minimizing its effect on the cable and hence its system impact. This objective involves designing a circuit and transducer tailored for PMN rather than using the PMN as a "drop-in" to a conventional lead zirconate titanate (PZT) transducer.

3. SUMMARY OF ACCOMPLISHMENTS

Our preliminary transducer design and modeling study has clearly shown that the significant advantage of PMN for broadband high-power-density transducer applications can be further augmented with different transducer designs such as graphite radiators. The added bandwidth complements the inherent material capability, allowing the 1 – 6 kHz frequency range to be covered using just two arrays. The PMN formulation being developed under this contract has already shown properties that will potentially exceed the performance available from types that already exist. Finally, using novel electronic circuit designs developed under this contract to eliminate the added power infrastructure for a PMN bias supply, we believe we can significantly reduce the ship impact of a system using these transducers by reducing the size of the cable and winch. This is achieved with creative use of transducer designs which accommodate the self-biasing requirements and thereby enable the large blocking capacitors to be eliminated.

The Phase-I program accomplishments are summarized below by program objective. More detail on the work performed and results obtained is presented in Sections 5 & 6.

PMN Formulation Development

On the basis of an extensive matrix of grain boundary enhancing compositions, we have been able to identify compositions where there is not only improved sintering behavior, but there is also much greater available strain with little effect on polarization hysteresis.

The electroceramics group at Alfred University has made excellent progress on the experimental matrix and a detailed report is given in Section 5. They have completed 13 trial compositions and the preliminary findings look very exciting. Notably, additions of Ti in combination with a counter-ion have produced up to 100% increases in strain without significant increases in polarization hysteresis. Other important results from the materials work include:

- sintered densities ~95% of theoretical were achieved
- the addition of Zn not only promotes grain growth as was expected but also is the most effective ion in increasing Tmax

- the addition of Ti alone did not increase Tmax or strain - counterions such as Ba, Sr (or Pb) are required

These findings are very exciting particularly because the results were obtained with more than one sample. Judging by this early quantitative data, the coating technique appears to be working well both in increasing strain and promoting sintering. The Alfred group intend to follow-up on these exciting findings even though the contract has ended -- albeit at a reduced level of effort.

Broadband Transducer Design Studies

We have conducted a survey of transducer classes and have succeeded in developing and modeling some very promising designs that show very adequate capability to cover the requisite bandwidth. Each transducer class required significant design iteration to optimize bandwidth and in some instances this resulted in dimensions, or other parameters, that violated conventional transducer design constraints. Classes that violated constraints or did not achieve the desired bandwidth were eliminated. The performances of the candidate designs are given in Section 6 and the more pertinent conclusions are summarized below.

Initial parametric studies on Class-IV flextensional transducers indicated a ~30% improvement in bandwidth can be achieved by using graphite-epoxy (GrEp) shells instead of aluminum (Al). Further improvements in bandwidth were obtained by increasing the ratio of the major to the minor axes (b/a) and the length of the shells.

Subsequent to the parametric studies, designs were prepared and evaluated for a variety of transducer types at the optimum frequency points. These optimum frequency point designs were selected to cover the frequency range 1 - 6 kHz with two transducers, i.e., one with a center frequency of ~1.7 kHz and the other centered at ~4.2 kHz. The designs were optimized based on results from the parametric study combined with other available data such as Navy models. The key findings are:

- the 1 - 6 kHz bandwidth can in principle be met with GrEp Class-IV and Class-VII flextensional designs or a GrEp moment bender
- the highest figure of merit (W/kg/kHz/Q) was obtained from the split cylinder design, but in order to achieve the bandwidth required, this transducer was unacceptably long (~2λ)
- The flexural disk design, which at first appeared promising, did not produce sufficient bandwidth

Bias Circuit Designs

In order to overcome a significant drawback in the use of PMN for high power density transducers -- the need for a separate bias supply -- we have been investigating electronic options that eliminate the large blocking capacitors and thus allow the relatively small bias electronics to be lowered into the wet end of the system. This effectively reduces the requirements on the cable (hence the winch system, hence the ship design) to be equivalent to a conventional piezoelectric system. Since this imposes a design constraint on the transducer requiring that the shell pairs be driven out of phase, novel transducer designs have been conceived to enable this mode of operation. At this point the GrEp flextensional and moment bender designs appear to be the most promising for the application based on bandwidth and power density (figure of merit). A combination Class-IV / Class-VII transducer is the leading contender to eliminate the blocking capacitor.

4. TECHNICAL FEASIBILITY

The approaches used in this Phase-I program have been specifically designed for manufacturing and deployment feasibility because in planning the program care was taken to include design, processing and materials amenable to implementation in an undersea transducer array. In particular:

- the coating method for the PMN material is readily amenable to scale-up using inexpensive materials and production equipment -- indeed the technique may even enhance productivity; and,
- the transducer designs and materials selected have been employed by the Navy or previously demonstrated by members of the Active Signal team -- this practicality was a criterion used in the study.

For the materials effort the most promising factor is that the tremendous strain improvements have been observed in several samples so we are confident that the effect is real. On the other hand, our long experience in this field reminds us that materials development is a long process and that even a reproducible laboratory result such as this is a relatively small step along the path. At this preliminary stage the most notable factors to be considered are:

- the strains have only been measured at room temperature, not at the lower temperatures where the strains are predicted to be much higher
- the measurements have only been conducted on small pellets
- a complete beginning-to-end reproducibility test has not yet been run

Overall, therefore, we rate the materials technology as technically feasible but with engineering work to be done. However, with the promise of increasing electrostrictive Q and potentially doubling strains (a 6-dB gain) it is a high-risk, high-payoff approach that ought to be pursued.

The feasibility of implementing the broadband transducer designs must be broken down into two categories:

1) broadband transducer designs; and
2) broadband transducer designs with accommodation made for out-of-phase stacks.

The straightforward Class-IV graphite-epoxy flextensional design for a broadband transducer has a very high probability of successful implementation. Not only have members of the Active Signal team designed, built and tested similar transducers in the past, but several of these units have also been in Navy service as communications transducers for a number of years. Furthermore, it should be noted that these designs have met the designated bandwidth requirement using the properties of currently-available PMN -- the materials under development herein will increase the power output and improve the electromechanical coupling. The combination transducer types designed to accommodate out-of-phase stacks and thus eliminate the blocking capacitor are untested and thus have to be assessed with a lower probability of implementation. A major challenge that we foresee is in the fabrication of a GrEp Class-VII shell because this shape is not readily amenable to direct winding on a mandrel.

In summary we believe that the approaches discussed are feasible, albeit with a range of difficulties in development. Moreover, we believe that the team of Active Signal and Alfred combined with

Lockheed Martin as a system implementation path is well qualified to demonstrate these technologies in hardware and we look forward to pursuing this in Phase II.

5. ELECTROMECHANICAL PROPERTIES OF MODIFIED PMN

5.1 Introduction

Many modified relaxor compositions based on $Pb(Mg_{1/3}Nb_{2/3})O_3$ ceramics (PMN's) have been developed to improve their dielectric and electrostrictive properties for various applications including actuators and transducers.[1-3] Several promising electromechanical properties like ~0.1% longitudinal strain (>0.3% transverse strain) at 1 kV/mm and 0.1 Hz, and <0.05 tanδ at weak field T_{max} and 1 kHz have been reported.[4-5] These properties constitute enabling performance for a wide variety of military and for commercial products.

Despite this demonstrated potential, the wide range in requirements of the potential applications has actually limited the use of PMN's. Since the applications are generally small volume and place very specific performance requirements on the ceramics, it would be great advantage if the compositions could be tailored to meet a given property specification. Such tailoring, after the majority of batch processing, would improve the economics of PMN manufacture and might also lead to improved understanding of the achievable properties in PMN.

This work presents a novel chemical way to achieve such tailoring by modifying a commercially available relaxor composition, $0.96(0.91Pb(Mg_{1/3}Nb_{2/3})O_3 - 0.09PbTiO_3) - 0.04\ BaTiO_3$. The chemical method is believed to result in an intimate mixing of small amounts of additives without an additional ball-mixing process. Thus since these additives are incorporated into the resultant ceramic by an unconventional means, the modified materials may not behave as simple compositionally altered materials.

Similar property modification has been demonstrated by other groups using unrelated materials and several particle coating processes. For example, coatings have been introduced to optimize microstructural control during densification for diverse purposes and applications.[6-10] Electronic ceramics or composite materials such as ferrites, $BaTiO_3$, $Y_1Ba_2Cu_3O_{7-\delta}$ superconductor, $Ni\text{-}Al_2O_3$ and $ZrO_2\text{-}Al_2O_3$ have been studied using the coating techniques. Of the methods, the sol-gel coating method has several advantages compared to the others. The gel tends to wet easily onto the surface of ceramic powder and thus can distribute additives homogeneously over the grain boundary region during sintering. The sol-gel coating procedure is appropriate when small amounts of additives or dopants are required to achieve an optimum performance of the resultant specimens through control of microstructural characteristics like grain size, pores and segregation.[6,8] Choice of additives for coating depends on the particular application and the type of material in question. After reviewing the potential dopants and modifiers for PMN's. the sol-gel approach was deemed the most promising.

A particle coating procedure was utilized in this PMN-PT-BT study. Several additives such as Ti, Zn, Fe, Sr and Ba were selected for the purpose of improving the properties of a given PMN-based composition. It will be seen that the coating procedure enhanced the homogeneity of additive distribution and the resultant properties. This final report demonstrates the particle coating procedure, and shows the resultant microstructures and properties of $0.96(0.91Pb(Mg_{1/3}Nb_{2/3})O_3 - 0.09PbTiO_3) - 0.04\ BaTiO_3$ sintered with the additives.

5.2 Experimental Procedure

5.2.1 Particulate Coating and Sintering

The flow chart of the experimental procedure is shown in Figure 1. A PMN-based composition of $0.96(0.91Pb(Mg_{1/3}Nb_{2/3})O_3 - 0.09PbTiO_3) - 0.04\ BaTiO_3$ was used in this work. The powder of $0.96(0.91Pb(Mg_{1/3}Nb_{2/3})O_3 - 0.09PbTiO_3) - 0.04\ BaTiO_3$ was supplied by NYSCC from stocks previously made by Martin Marietta Laboratories. The powder was first milled in ethyl-alcohol using yttria-stabilized zirconia balls for 20 hr.

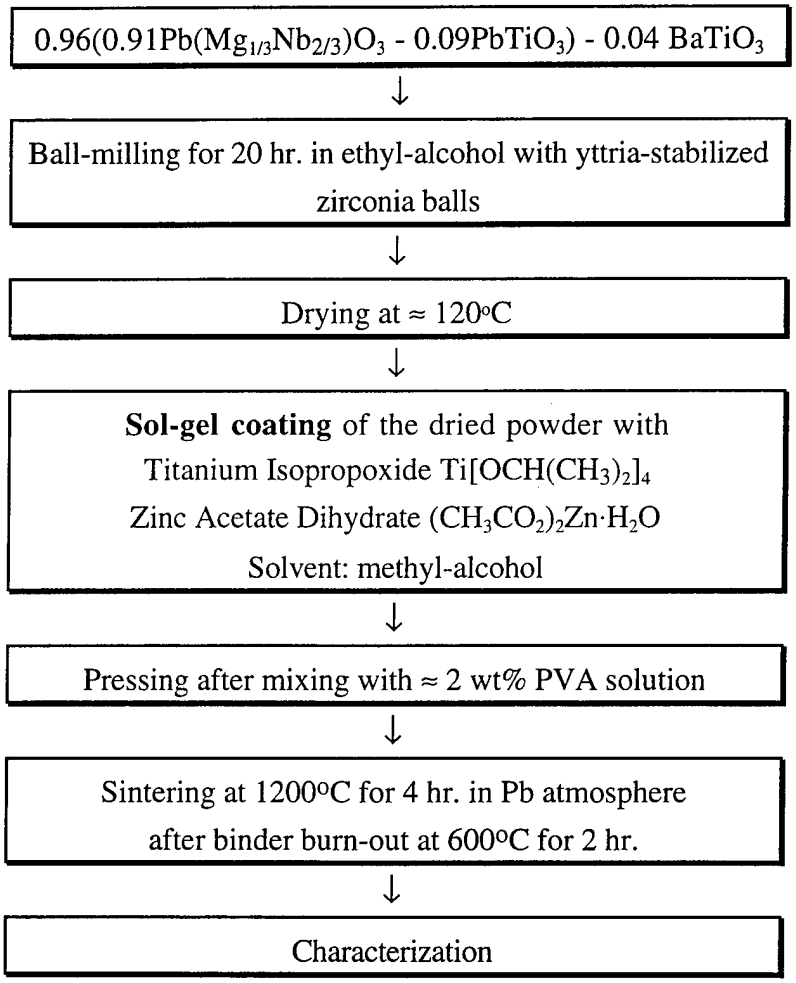

Figure 1. Flow chart of the sol-gel coating process

A particulate coating procedure was utilized to incorporate additives such as Ti, Zn, Fe, Ba and Sr into the base powder. The compositions of the additives are represented in Table I. All the additives contain TiO_2. Titanium isopropoxide $Ti[OCH(CH_3)_2]_4$, zinc acetate dihydrate $(CH_3CO_2)_2Zn{\cdot}H_2O$, iron (III) acetylacetonate $[CH_3COOH{=}C(O\text{-})CH_3]_3Fe$, strontium acetate $(CH_3CO_2)_2Sr$ and barium acetate $(CH_3CO_2)_2Ba$ were used as raw materials for the additives.

Titanium isopropoxide was first dissolved in isopropanol, and then Zn acetate or Fe acetylacetonate was added into the solution. A tiny amount of nitric acid was used as a catalyst to precipitate the sol-gel reaction. In the cases of the additives including Sr and Ba, an aqueous solution of the Sr or Ba acetate was prepared and then mixed with a partially-hydrolyzed Ti isopropoxide solution in isopropanol. Immediate gelation was observed after mixing.

Table 1. Additive compositions, and bulk density values of the $0.96(0.91Pb(Mg_{1/3}Nb_{2/3})O_3 - 0.09PbTiO_3) - 0.04\ BaTiO_3$ samples sintered at 1200°C for 4 hr.

Sample ID	Additive Composition	Bulk Density (g/cm^3)
PM-1	no additives, as-received	-
PM-2	no additives, ball-milled	7.64
PM-3	0.5 wt% TiO_2 & 0.5 wt% ZnO	7.75
PM-4	0.5 wt% TiO_2 & 2 wt% ZnO	7.71
PM-5	2 wt% TiO_2 & 2 wt% ZnO	7.65
PM-6	0.5wt% TiO_2	7.86
PM-7	0.5 wt% TiO_2 & 0.5 wt% Fe_2O_3	7.72
PM-8	0.5 wt% TiO_2 & 0.5 wt% BaO	7.83
PM-9	0.5 wt% TiO_2, 0.5 wt% BaO & 0.5 wt% Fe_2O_3	7.67
PM-10	0.5 wt% TiO_2, 0.5 wt% ZnO & 0.5 wt% Fe_2O_3	7.59
PM-11	0.5 wt% TiO_2, 0.5 wt% ZnO & 0.5 wt% BaO	7.61
PM-12	0.5 wt% TiO_2 & 0.5 wt% SrO	7.68
PM-13	0.5 wt% TiO_2, 0.5 wt% ZnO & 0.5 wt% SrO	7.63

The ball-milled PMN-PT-BT powders were inserted into each solution containing the additives while the solution was stirred with a magnetic bar. The stirring process was continued until the complete evaporation of the solvent took place at room temperature. A gel reaction was believed to occur during this evaporation in the cases which do not contain Sr and Ba. The final rigid powders containing a gel of the additives were crushed using a mortar/pestle. After mixing with a 2 wt% PVA aqueous solution, pressing was conducted at ≈ 10,000 psi to make disk-shaped pellets (diameter = 15 mm). For example, 0.1g of the binder solution was added to 1.5 g of the powder. The pressed pellets were sintered at 1200°C for 4 hr. in Pb atmosphere (using calcined $PbZrO_3$ + 5 wt% ZrO_2 powders) after burn-out of organics from the raw materials and binder at 600°C for 2 hr.

5.2.2 Characterization and Property Evaluation

The phase before and after the ball-milling was identified by an X-ray diffractometer. The coated powder was investigated by using a transmission electron microscope (2000FX, JEOL Co.). Several drops of acetone solution containing the coated powders were dripped onto a copper TEM grid coated with an evaporated carbon film. TEM was operated at 120 kV. For the microstructure

observation of the fracture surface of the sintered specimens, a scanning electron microscope (1810 SEM, Amray Co.) was used. Bulk density was measured by using the Archimedes' principle in deionized water.

The sintered pellets were electroded with silver paste after sputtering both sides of the samples with Pd-Ag. These electrodes were then fired at 550°C for 1 hr. Dielectric properties of the sintered samples were measured using an LCR meter (HP4284A) with variations in frequency and temperature. A modified Sawyer-Tower circuit was used to observe polarization behavior with electric field. In the case of longitudinal strain measurement, a Fotonic™ Sensor (MTI 2000 Fotonic Sensor) was used. The strain and polarization measurements were conducted at room temperature. The set-up for the polarization and strain measurements included a multifunction synthesizer (HP8904A), a high-voltage amplifier (Model 609D, Trek Co.) and a analog/digital converter (ADC488/85A) connected to a PC--all driven by LabView™ computer routines.

5.3 Results and Discussion

5.3.1 Particulate Coating with Additives

Figure 2 shows the powder characteristics of the base PMN-PT-BT after ball-milling (before sol-gel coating). Particle size seems to be fairly uniform and less than 1 μm. It should be mentioned that some aggregates were found to exist in the powder. Phase-pure perovskite was observed for the base powder regardless of the ball-milling process as noted in the XRD patterns of Fig. 3.

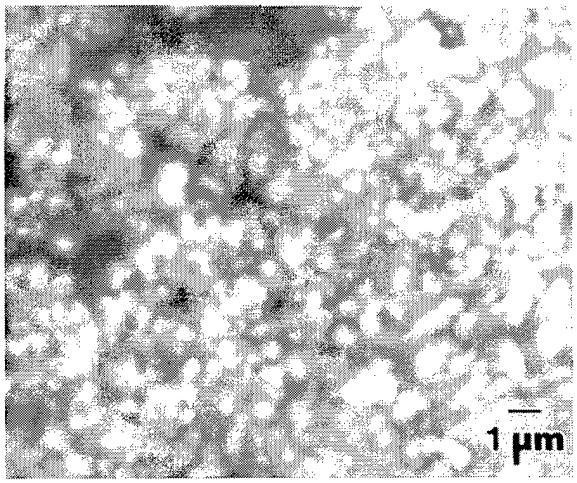

Figure 2. SEM of $0.96(0.91Pb(Mg_{1/3}Nb_{2/3})O_3 - 0.09PbTiO_3) - 0.04\ BaTiO_3$ powder before sol-gel coating

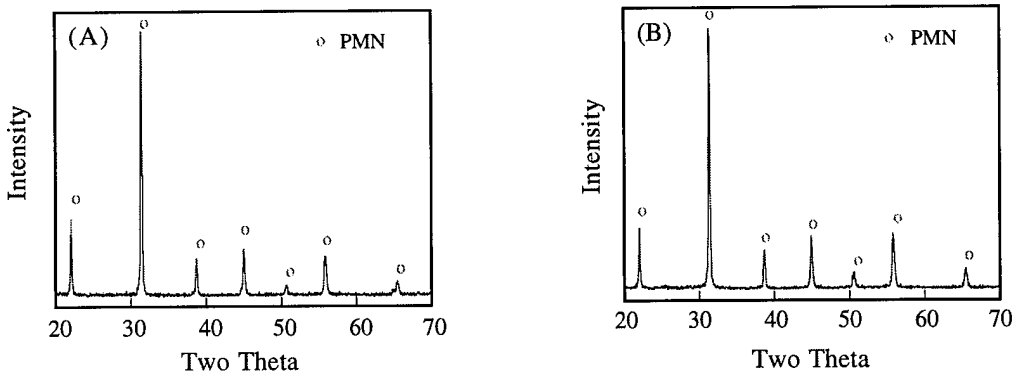

Figure 3. XRD patterns of $0.96(0.91Pb(Mg_{1/3}Nb_{2/3})O_3 - 0.09PbTiO_3) - 0.04\ BaTiO_3$ powder (A) before ball-milling and (B) after ball-milling.

The deposition of the gel additives on the particle surface was observed directly. For example, a coating layer consisting of Zn and Ti (corresponding to a additive composition, 0.5 wt% ZnO and 0.5 wt% TiO_2) was seen in nanoscale on the surface of the PMN-PT-BT particles as shown in the TEM micrograph of Fig. 4 (A). Arrows in this figure indicate the layer. A relatively uniform coating of the sol-gel materials was observed. Since the viscosity of the gel is expected to decrease as temperature increases, structures such as those in Fig. 4(A) should result in uniformly distributed layers during sintering. The layer was identified as a gel as shown in the XRD pattern of Fig. 4(B). For the XRD, a gel of Zn and Ti was prepared without PMN-PT-BT powder under the same experimental condition.

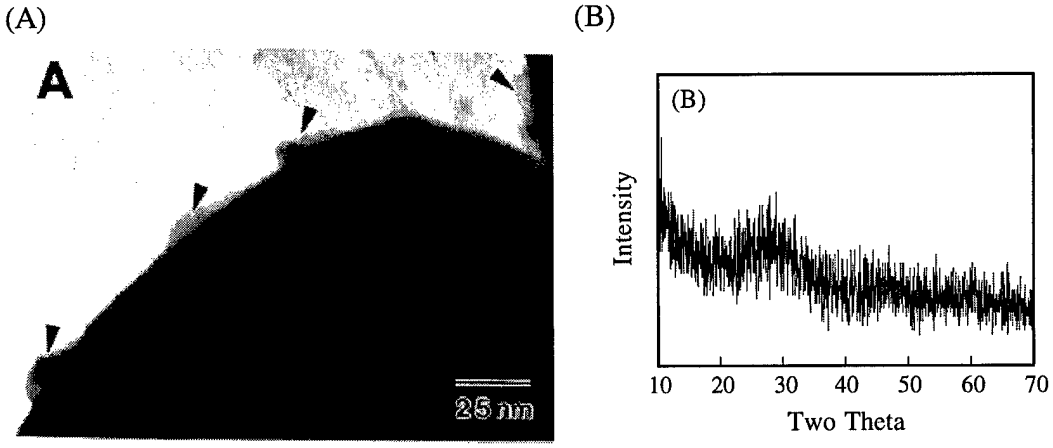

Figure 4. (A) TEM micrograph showing a sol-gel coated layer on the surface of $0.96(0.91Pb(Mg_{1/3}Nb_{2/3})O_3 - 0.09PbTiO_3) - 0.04\ BaTiO_3$ particles, and (B) XRD pattern of the dried gel consisting of Ti and Zn.

5.3.2 Densification and Microstructures

Table 1 represents bulk density values of the samples containing different additives. Most of the additives tended to increase the density values compared to the value (7.64 g/cm^3) for the samples

without the additives. However, a higher Zn and Ti content showed a decrease in the density value as evident from the values of PM-3 to PM-5. The addition of Fe and Ba appear to be directly in enhancing the fired density. The highest value, 7.86 g/cm^3 was obtained in the case (PM-6) of 0.5 wt% TiO_2 addition. In all cases, the green density was in the range 60 to 62 % of the theoretical one (8.13g/cm^3).

Figs. 5 and 6 show the fracture surfaces of the samples sintered at 1200°C for 4 hr. with the chemical additives. The microstructural characteristics were found to depend on the additive compositions. Ti appears to inhibit the grain growth as shown from Fig. 5(A) to Fig. 5(E). An increase in the content of Zn was found to aid grain growth as evident in the microstructure change from Fig. 5(B) to Fig. 5(C). Fe was also found to enhance grain growth. On the other hand, Ba and Sr did not seem to significantly affect grain growth. It should be also noted that the intergranular fracture tended to disappear with some additives (for example, as seen clearly in Fig. 6 (D)), indicating a change in grain-boundary nature. The relatively uniform grain size distribution in the microstructures suggest the homogeneous distribution of the chemically-derived additives.

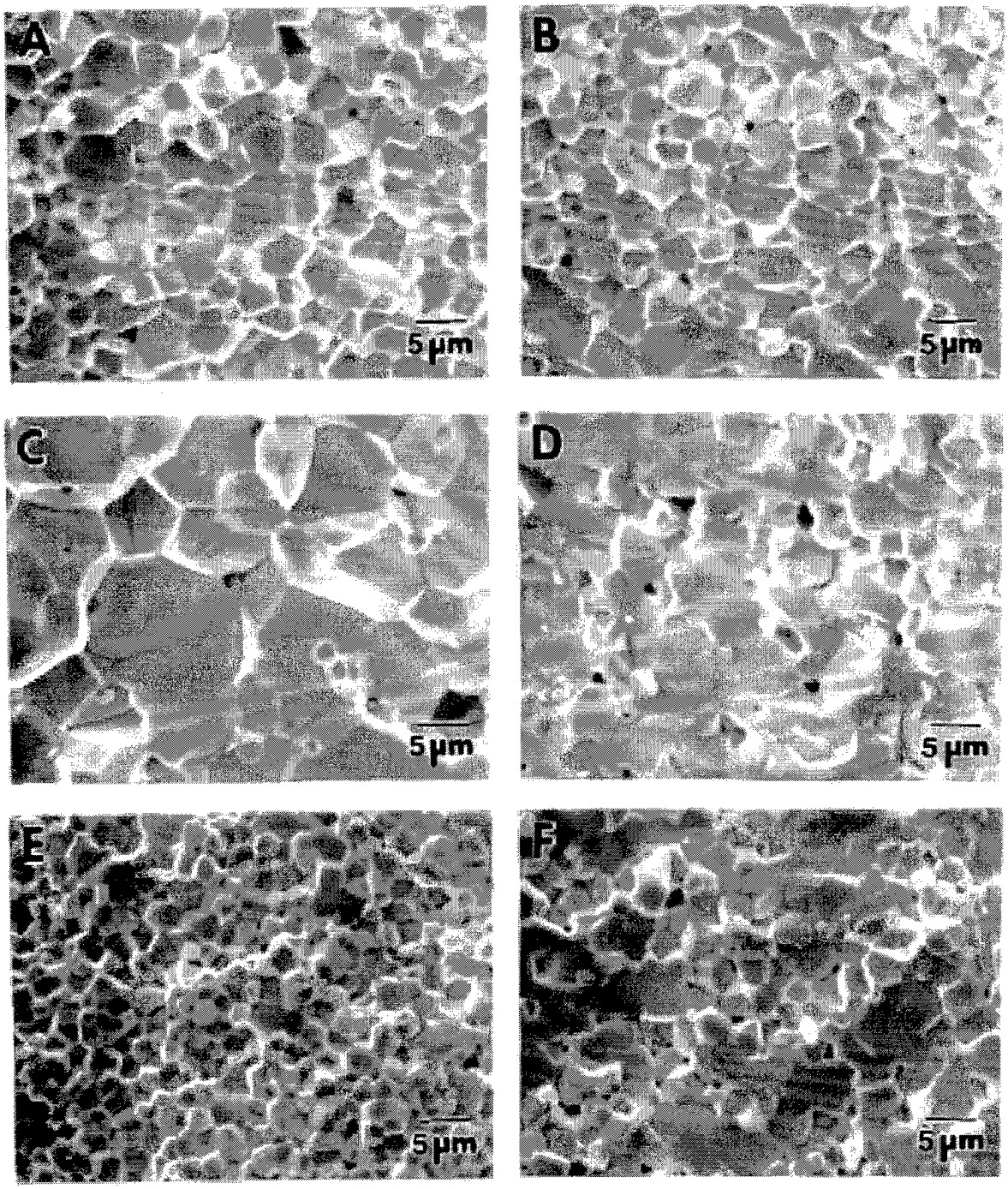

Figure 5. Microstructures of $0.96(0.91Pb(Mg_{1/3}Nb_{2/3})O_3 - 0.09PbTiO_3) - 0.04\ BaTiO_3$ samples with additives, sintered at 1200°C for 4 hr.: (A) PM-2 (B) PM-3, (C) PM-4, (D) PM-5, (E) PM-6 and (F) PM-7.

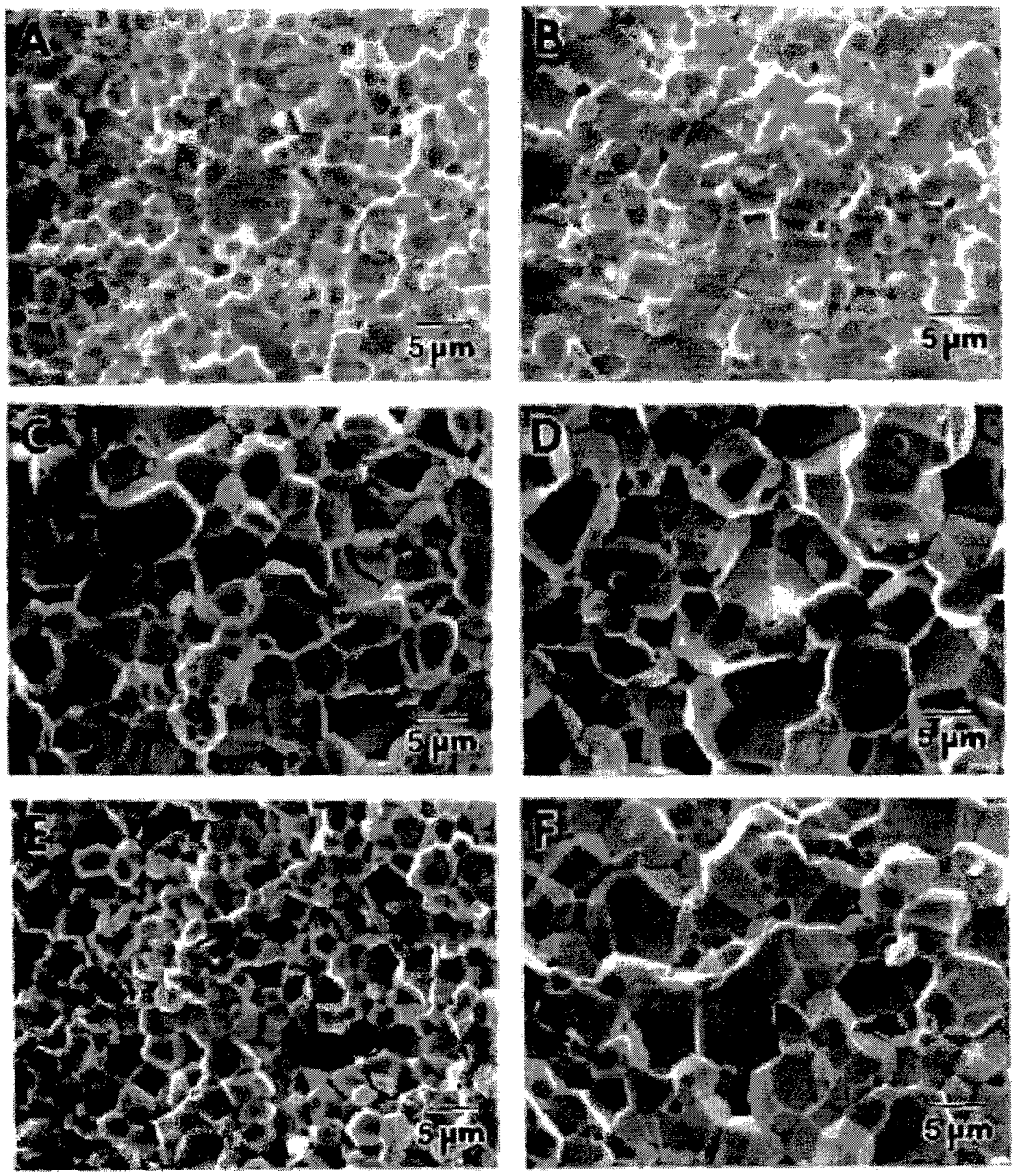

Figure 6. Microstructures of $0.96(0.91Pb(Mg_{1/3}Nb_{2/3})O_3 - 0.09PbTiO_3) - 0.04\ BaTiO_3$ samples with additives, sintered at 1200°C for 4 h: (A) PM-8 (B) PM-9, (C) PM-10, (D) PM-11, (E) PM-12, (F) PM-13.

5.3.3 Dielectric and Weak-field Properties

Figs. 7 to 13 show the variations in dielectric constant (k') and loss tangent (tanδ) with temperature (T) and frequency according to different additives. The several specific values like k'_{max}, k' at RT, tanδ at room temperature, tanδ at k'_{max} and T of k'_{max} which were obtained from the plots are represented in Table II.

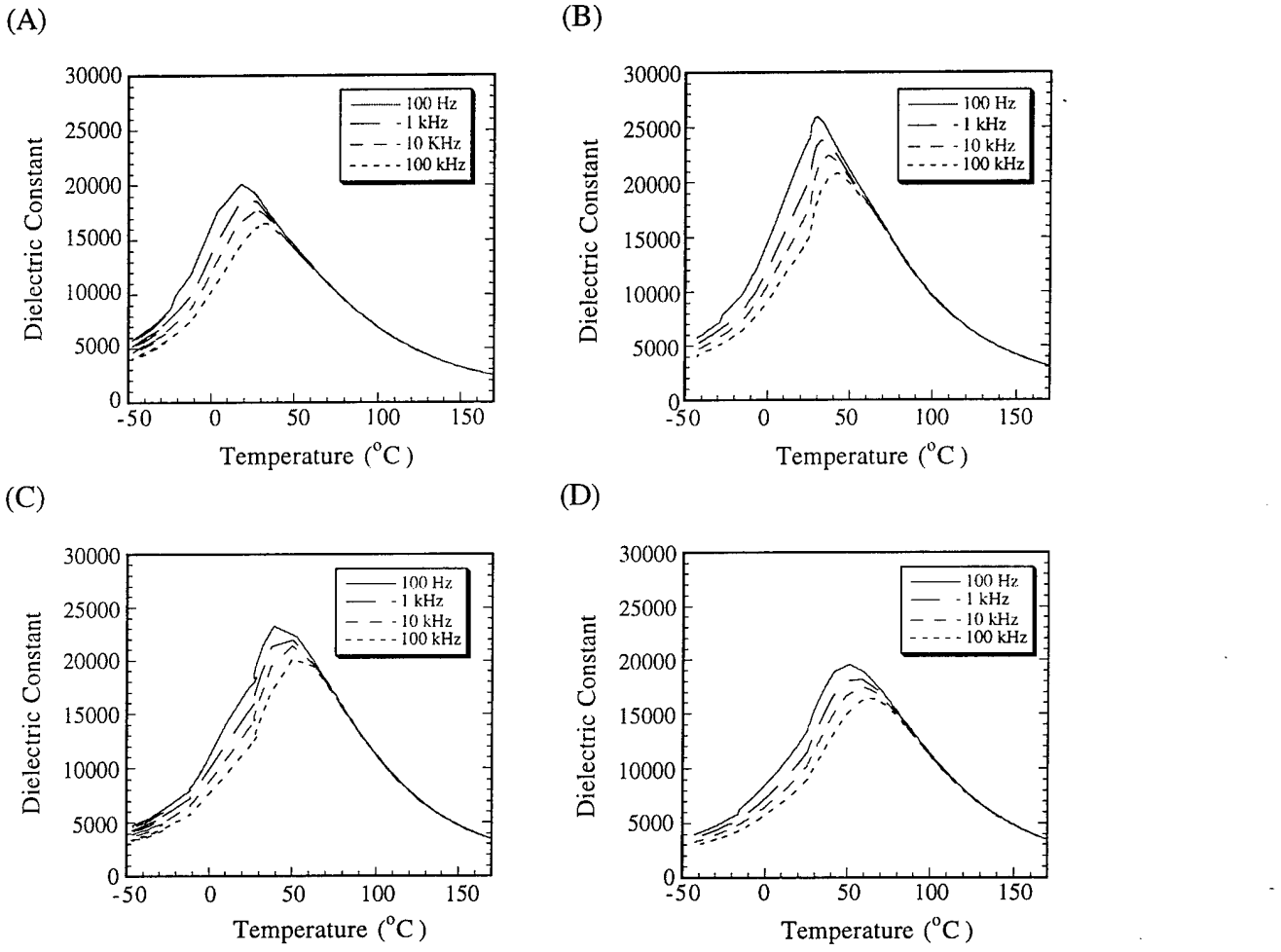

Figure 7. Plots of permittivity vs temperature for $0.96(0.91Pb(Mg_{1/3}Nb_{2/3})O_3 - 0.09PbTiO_3) - 0.04\ BaTiO_3$ samples with additives, sintered at 1200°C for 4 h: (A) PM-2, (B) PM-3, (C) PM-4 and (D) PM-5.

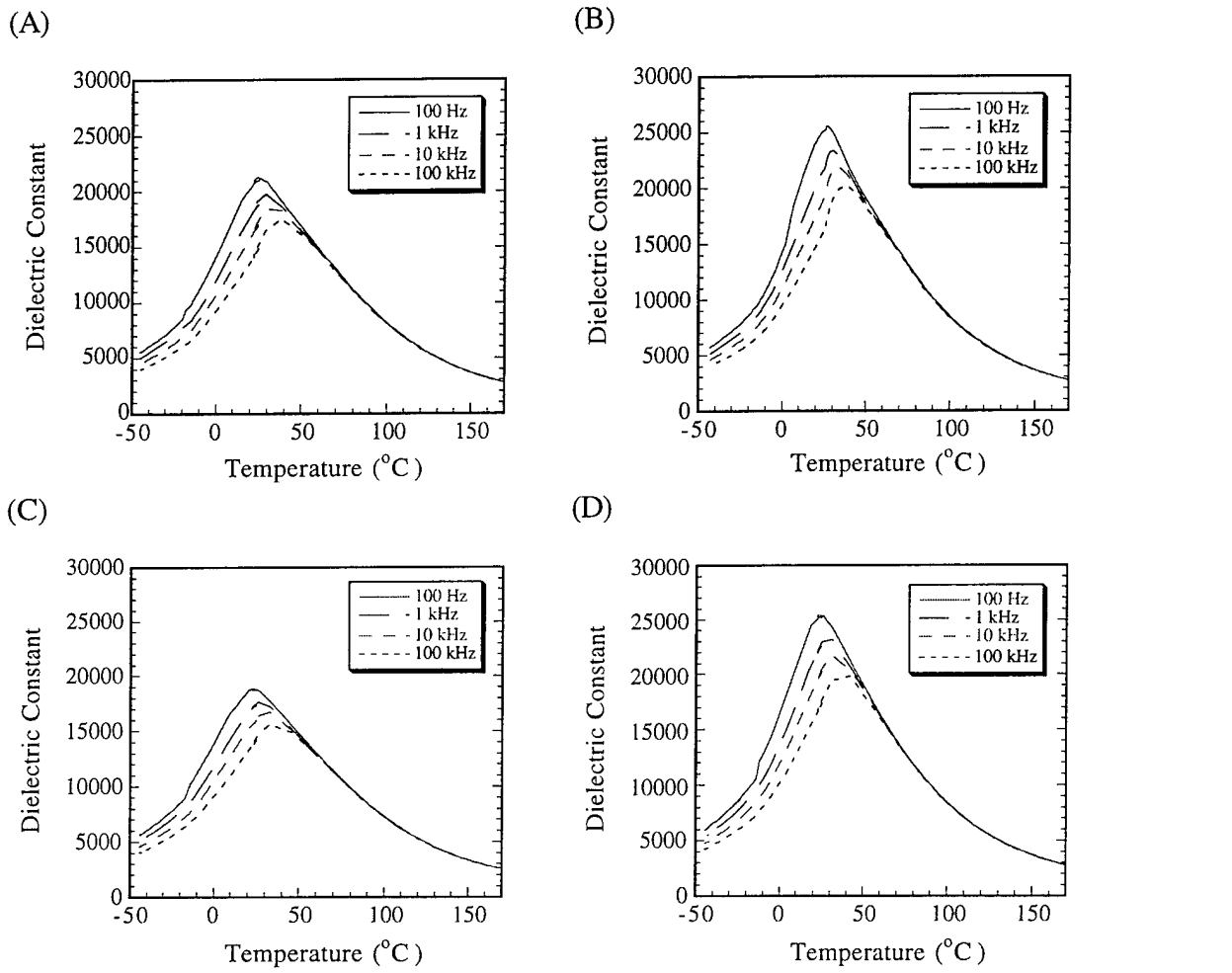

Figure 8. Plots of permittivity vs. temperature for $0.96(0.91Pb(Mg_{1/3}Nb_{2/3})O_3 - 0.09PbTiO_3) - 0.04 BaTiO_3$ samples with additives, sintered at 1200°C for 4 h: (A) PM-6, (B) PM-7, (C) PM-8 and (D) PM-9.

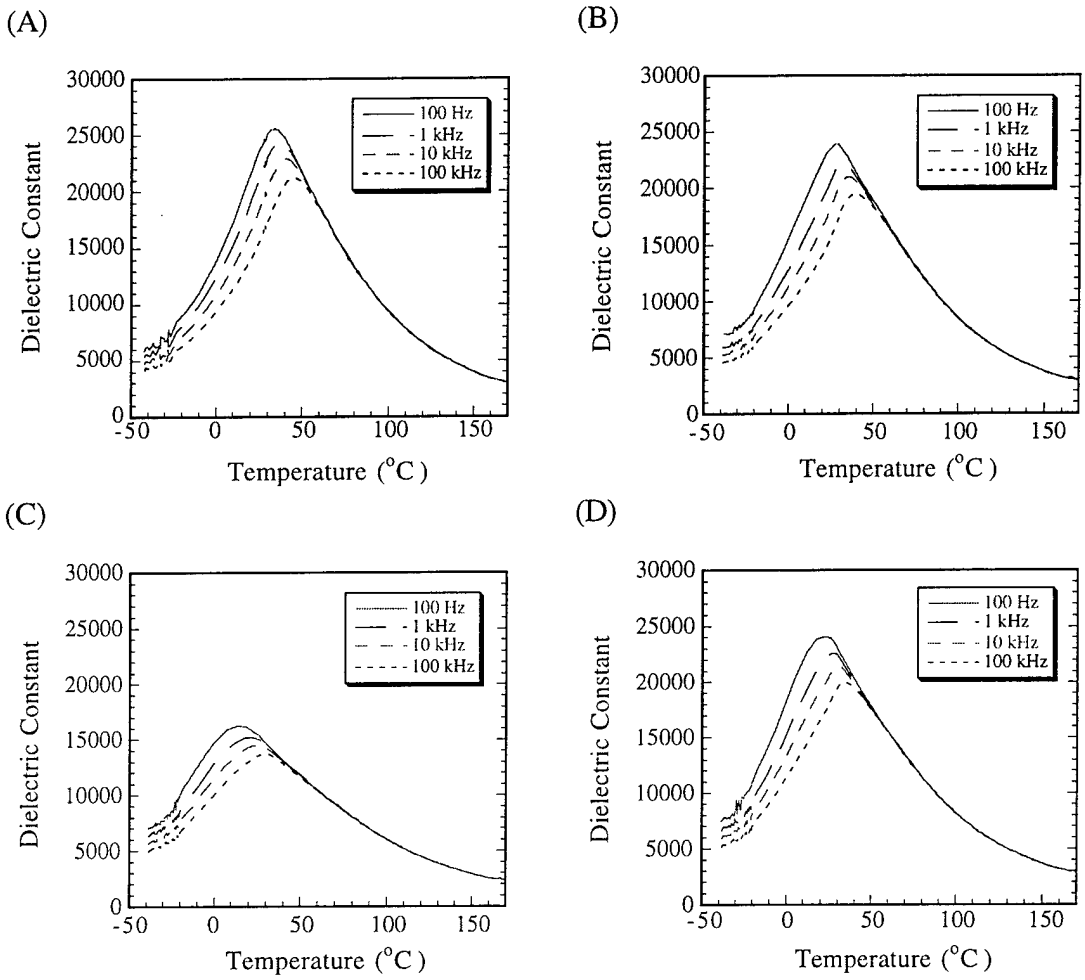

Figure 9. Plots of permittivity vs. temperature for $0.96(0.91Pb(Mg_{1/3}Nb_{2/3})O_3 - 0.09PbTiO_3) - 0.04 BaTiO_3$ samples with additives, sintered at 1200°C for 4 h: (A) PM-10, (B) PM-11, (C) PM-12 and (D) PM-13.

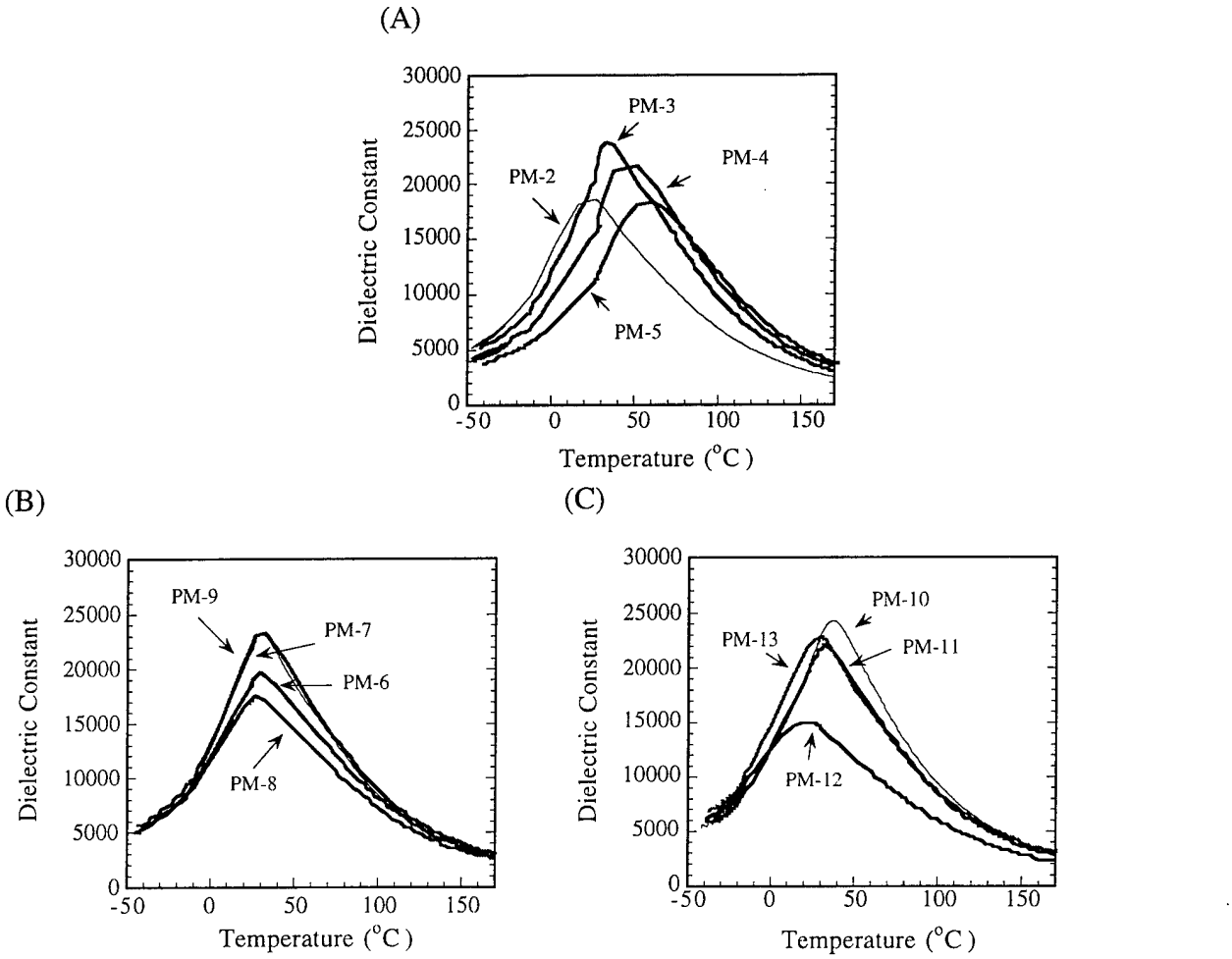

Figure 10. Plots of dielectric constant (at 1 kHz) vs. temperature for $0.96(0.91Pb(Mg_{1/3}Nb_{2/3})O_3 - 0.09PbTiO_3) - 0.04\ BaTiO_3$ samples with additives, sintered at 1200°C for 4 hr.: (A) PM-2 to PM-5, (B) PM-6 to PM-9 and (C) PM-10 to PM-13.

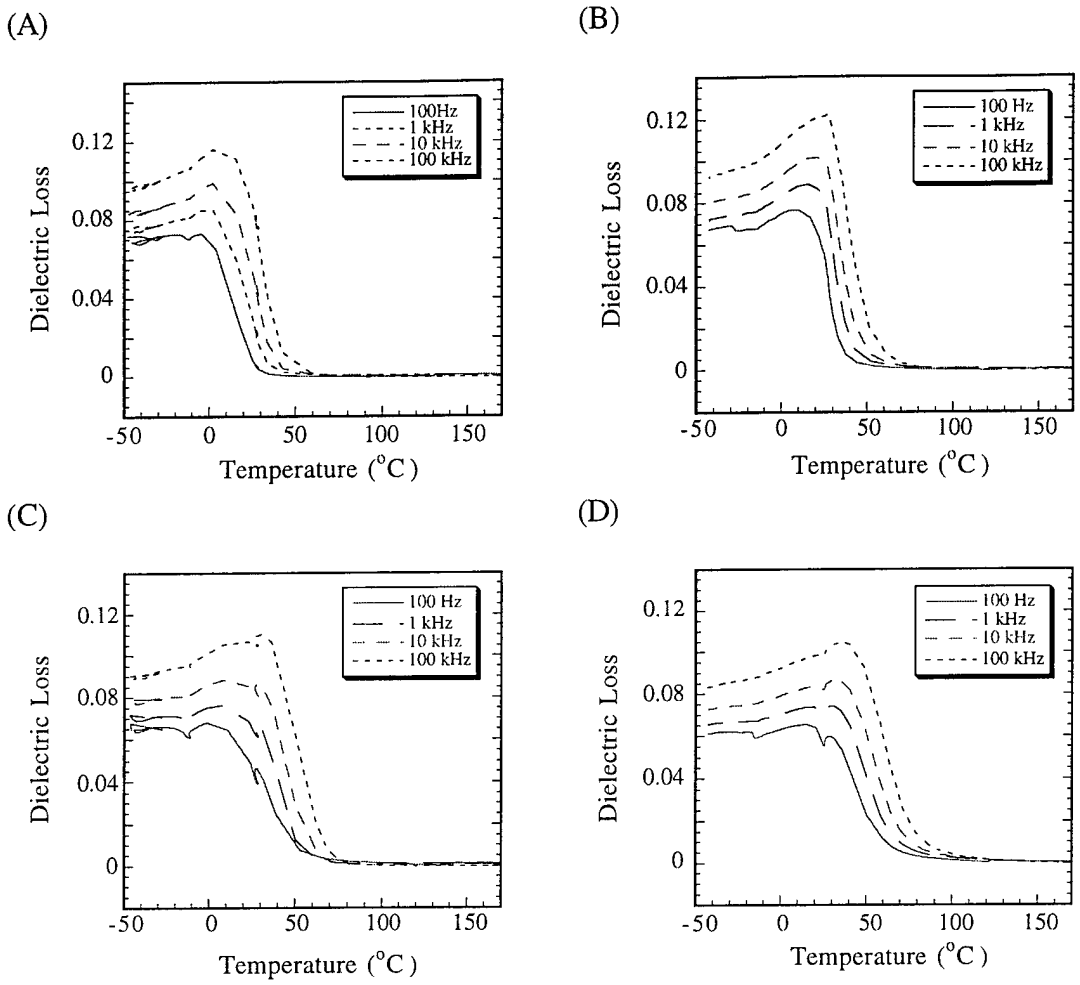

Figure 11. Plots of dielectric loss vs. temperature for $0.96(0.91Pb(Mg_{1/3}Nb_{2/3})O_3 - 0.09PbTiO_3) - 0.04 BaTiO_3$ samples w. additives, sintered at 1200°C for 4 h: (A) PM-2, (B) PM-3, (C) PM-4 and (D) PM-5.

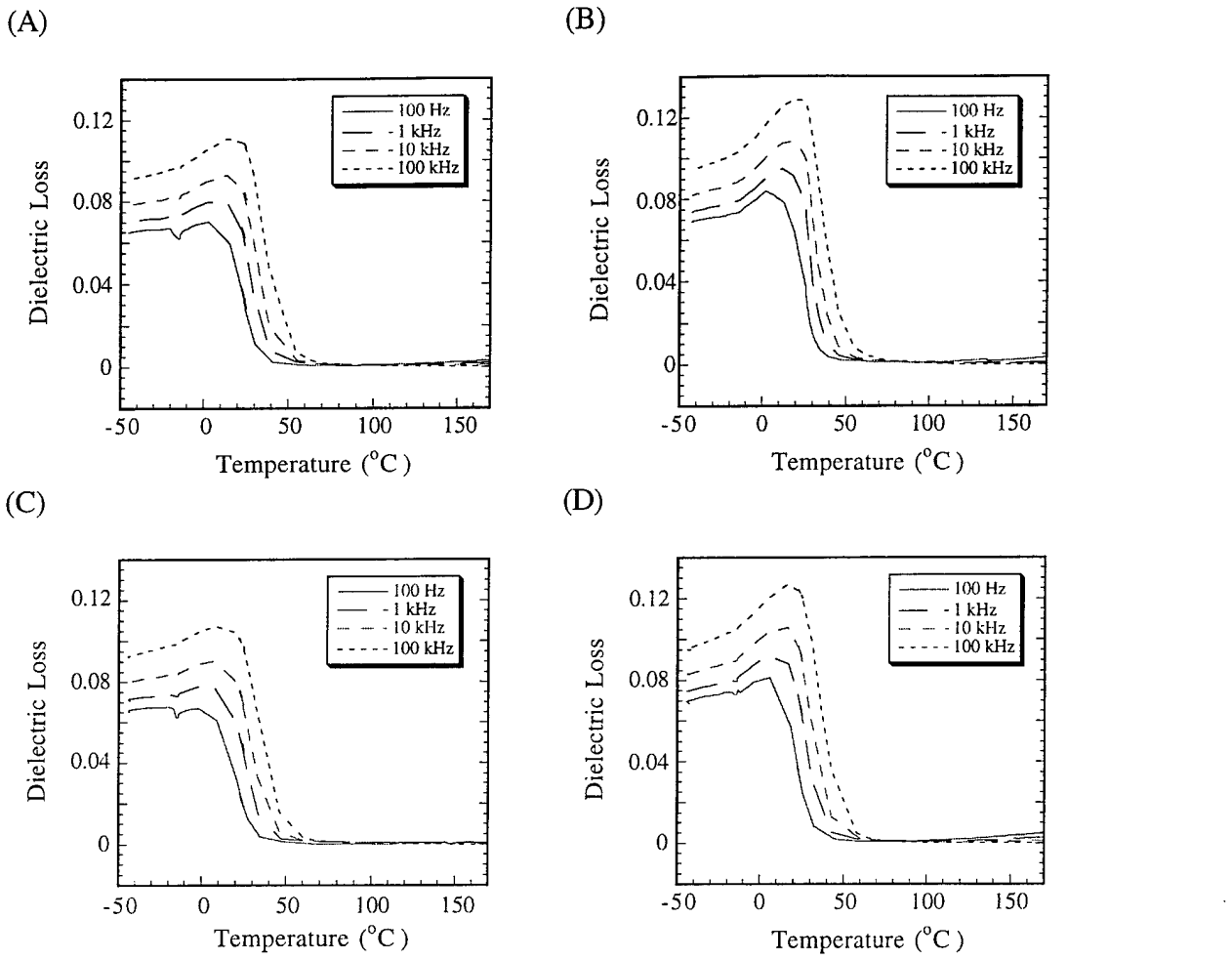

Figure 12. Plots of dielectric loss vs. temperature for $0.96(0.91Pb(Mg_{1/3}Nb_{2/3})O_3 - 0.09PbTiO_3) - 0.04 BaTiO_3$ samples with additives, sintered at 1200°C for 4 h: (A) PM-6, (B) PM-7, (C) PM-8 and (D) PM-9.

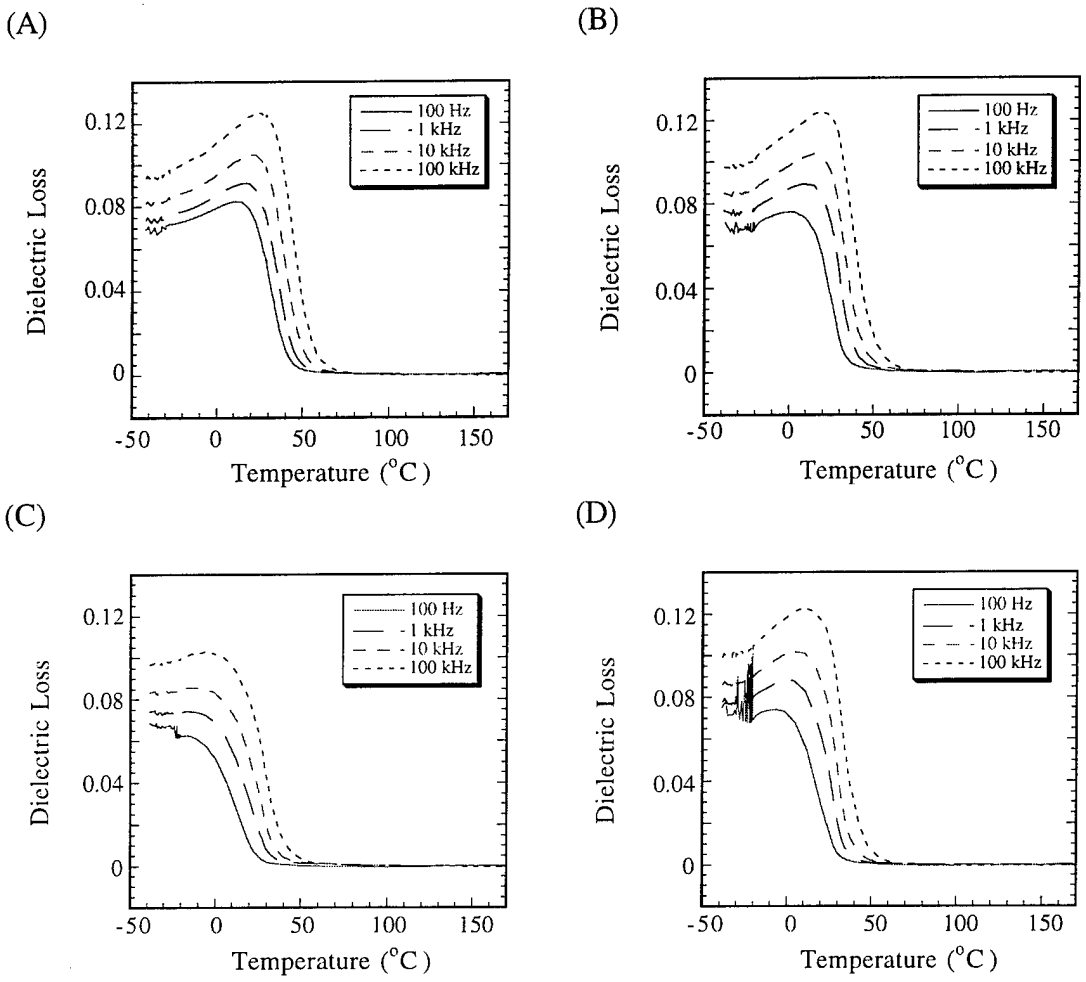

Figure 13. Plots of dielectric loss vs. temperature for $0.96(0.91Pb(Mg_{1/3}Nb_{2/3})O_3 - 0.09PbTiO_3) - 0.04 BaTiO_3$ samples with additives, sintered at 1200°C for 4 h: (A) PM-10, (B) PM-11, (C) PM-12 and (D) PM-13.

Table 2. Dielectric properties (at 1 kHz) of the $0.96(0.91Pb(Mg_{1/3}Nb_{2/3})O_3 - 0.09PbTiO_3) - 0.04\ BaTiO_3$ samples with additives, sintered at 1200°C for 4 h.

Sample ID	k' at RT*	tanδ at RT	k'_{max}	tanδ at k'_{max}	Temp at k'_{max}
PM-2	18,600	0.029	18,600	0.029	25°C
PM-3	20,200	0.082	23,800	0.044	32°C
PM-4	15,500	0.065	21,900	0.012	50°C
PM-5	11,500	0.070	18,200	0.023	59°C
PM-6	18,800	0.050	19,800	0.036	29°C
PM-7	22,000	0.077	23,400	0.039	30°C
PM-8	17,400	0.045	17,600	0.038	26°C
PM-9	22,600	0.063	23,200	0.031	31°C
PM-10	21,600	0.084	24,300	0.032	38°C
PM-11	20,800	0.070	22,200	0.037	31°C
PM-12	15,100	0.019	15,200	0.030	21°C
PM-13	22,400	0.046	22,600	0.040	26°C

* RT: room temperature ≈ 25°C

Most striking in Table 2 is the significant variation of k'_{max} and T of k'_{max} for the various compositions. Specifically PM-3, PM-8, and PM-13 show significant increases in permittivity without an accompanying shift in peak performance or significant trend in density. These variations are well outside the changes expected from prior work with different compositions of PMN. This supports the original hypothesis that modification by sol-gel is *different* than a conventional modification of composition. It promotes improved dielectric response which cannot be simply ascribed to density or composition. It appears to arise from direct modification of the grain boundary or grain surfaces.

5.3.4 Electromechanical Properties

The electromechanical properties shown in Table III and in Figs. 14 to 19 also provide significant information. Aging of the polarization response can be noted in some compositions, e.g., PM-4 in Fig. 14C. This continues to support the existence of a rough correlation between enlarged grain size and the existence of aging in PMN's. The influence of varied T of k'_{max} can also be seen in the polarization data. However, more significant from a practical standpoint are the peak polarizations of PM-3, PM-8, and PM-13 that approximate that of the base composition. These three compositions have T of k'_{max} very near the base composition, yet show significantly different polarization behavior in terms of saturation at 1 kV/mm. PM-8 shows only the barest beginnings of polarization saturation.

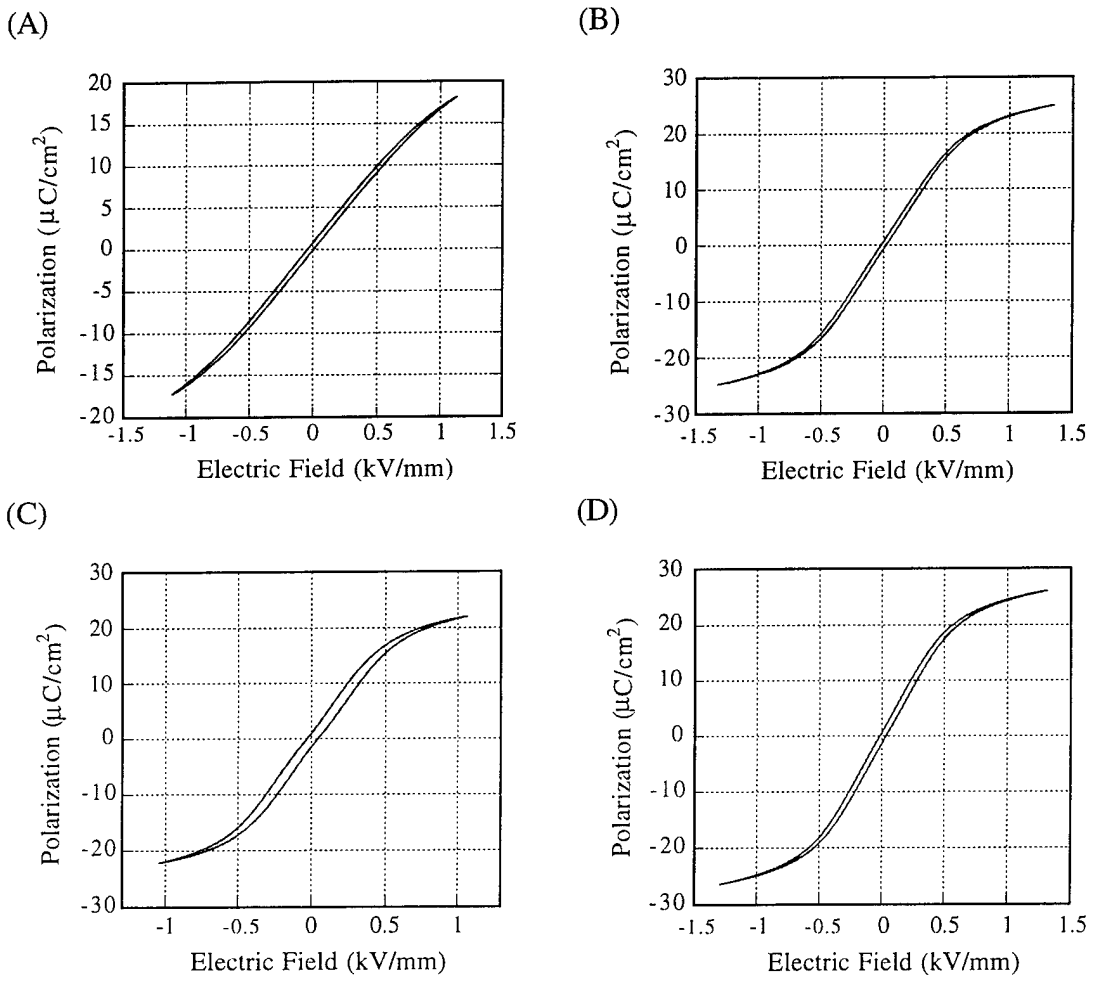

Figure 14. Plots of polarization vs. temperature for $0.96(0.91Pb(Mg_{1/3}Nb_{2/3})O_3 - 0.09PbTiO_3) - 0.04 BaTiO_3$ samples w. additives, sintered at 1200°C for 4 h: (A) PM-2, (B) PM-3, (C) PM-4 and (D) PM-5.

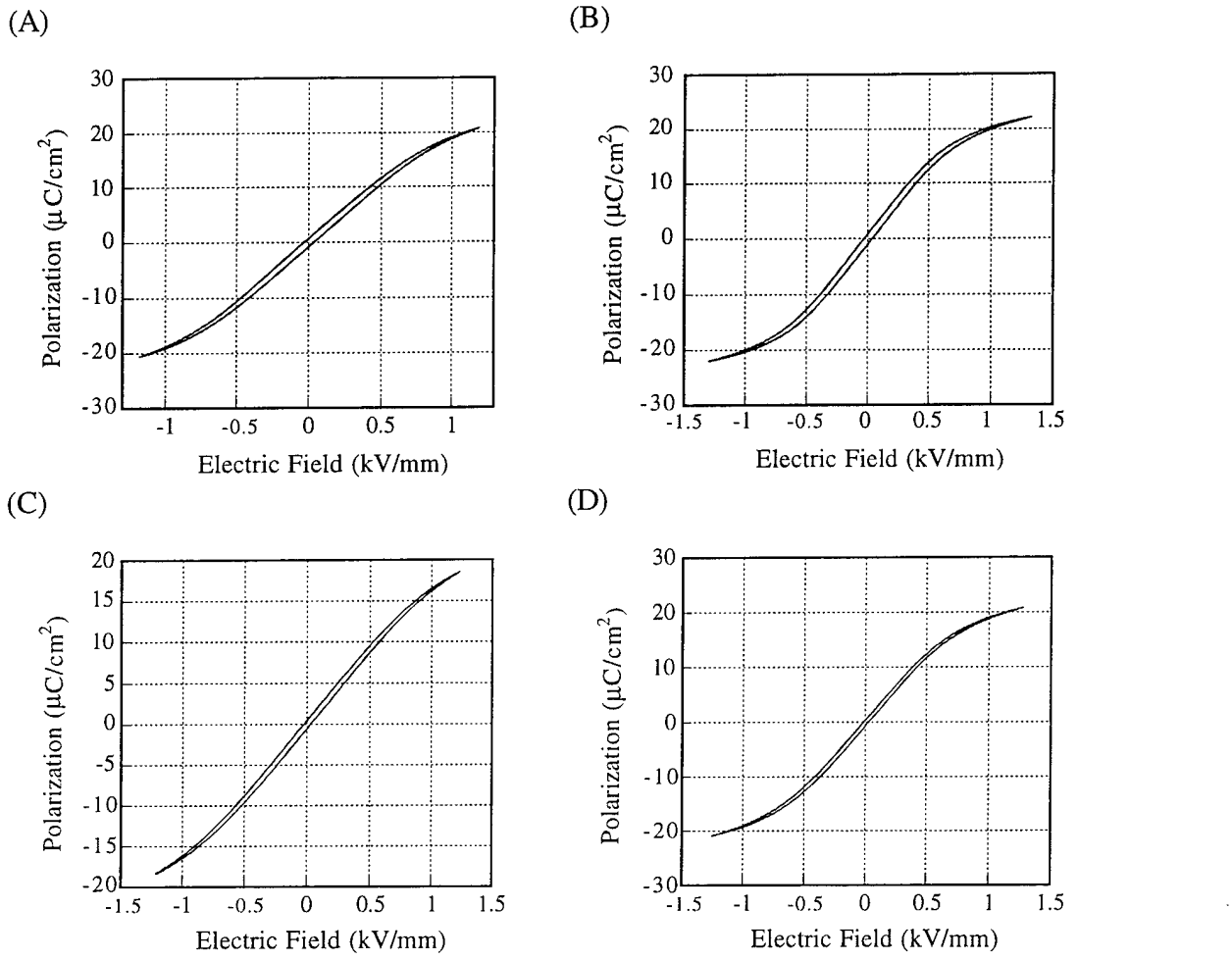

Figure 15. Plots of polarization vs. temperature for $0.96(0.91Pb(Mg_{1/3}Nb_{2/3})O_3 - 0.09PbTiO_3) - 0.04 BaTiO_3$ samples with additives, sintered at 1200°C for 4 h: (A) PM-6, (B) PM-7, (C) PM-8 and (D) PM-9.

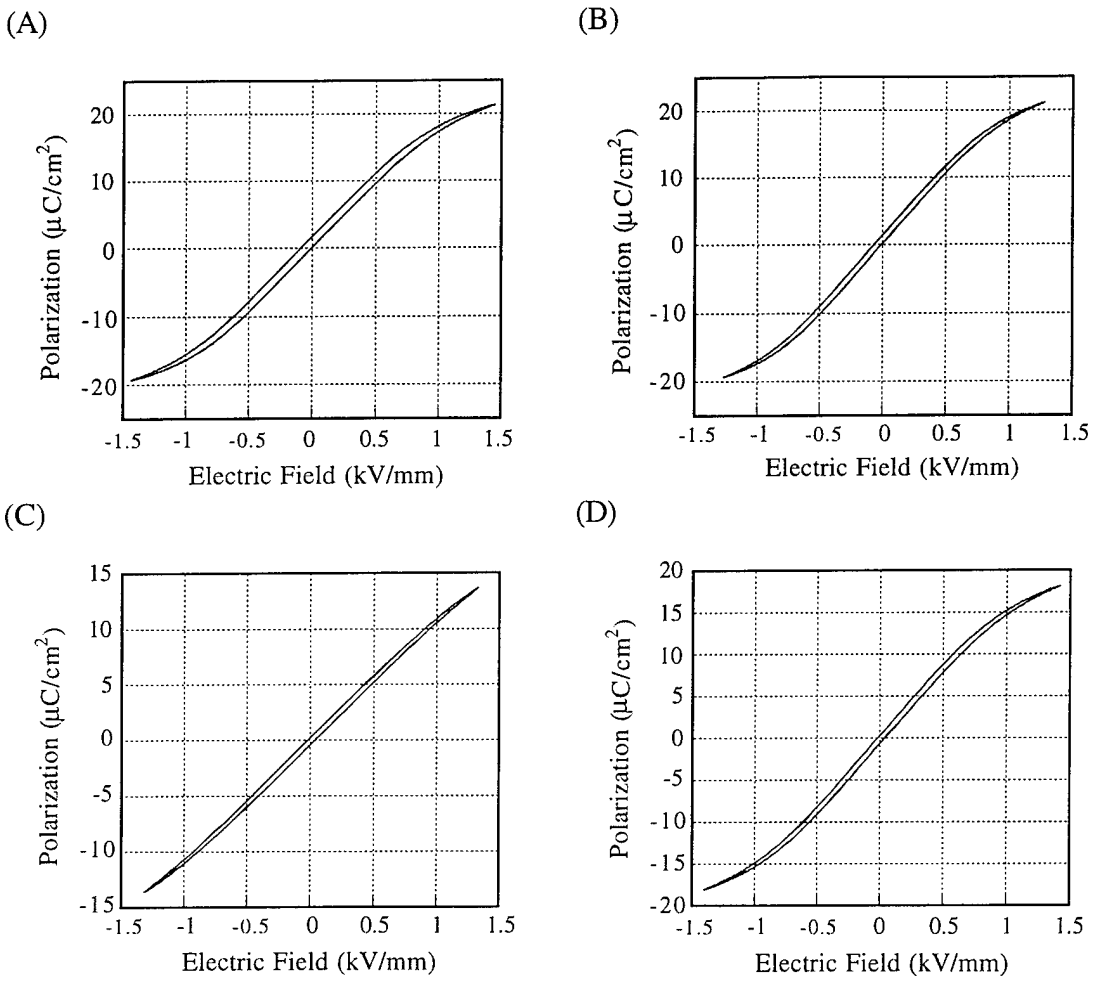

Figure 16. Plots of polarization vs. temperature for $0.96(0.91Pb(Mg_{1/3}Nb_{2/3})O_3 - 0.09PbTiO_3) - 0.04 BaTiO_3$ samples with additives, sintered at 1200°C for 4 h: (A) PM-10, (B) PM-11, (C) PM-12 and (D) PM-13.

Table 3. Electromechanical properties of the $0.96(0.91Pb(Mg_{1/3}Nb_{2/3})O_3 - 0.09PbTiO_3) - 0.04\ BaTiO_3$ samples with additives, sintered at 1200°C for 4 h.

Sample ID	Micro Strain* at ≈ 1 kV/mm	Polarization* ($\mu C/cm^2$) at ≈ 1 kV/mm
PM-2	≈ 220	17
PM-3	≈ 440	23
PM-4	≈ 290	22
PM-5	≈ 390	25
PM-6	≈ 110	19
PM-7	≈ 290	20
PM-8	≈ 480	17
PM-9	≈ 400	19
PM-10	≈ 350	18
PM-11	≈ 290	18
PM-12	≈ 80	11
PM-13	≈ 490	15

* measured at room temperature ≈ 25°C

All three show *twice* the strain of the base material at an identical field (Fig. 17, 18, 19) with an unexpected increase in apparent electrostrictive *Q*-coefficient (Table 3). Although not presently understood, this is a double bonus for electromechanical uses--the output strain increases without a corresponding increase in the electrical drive energy

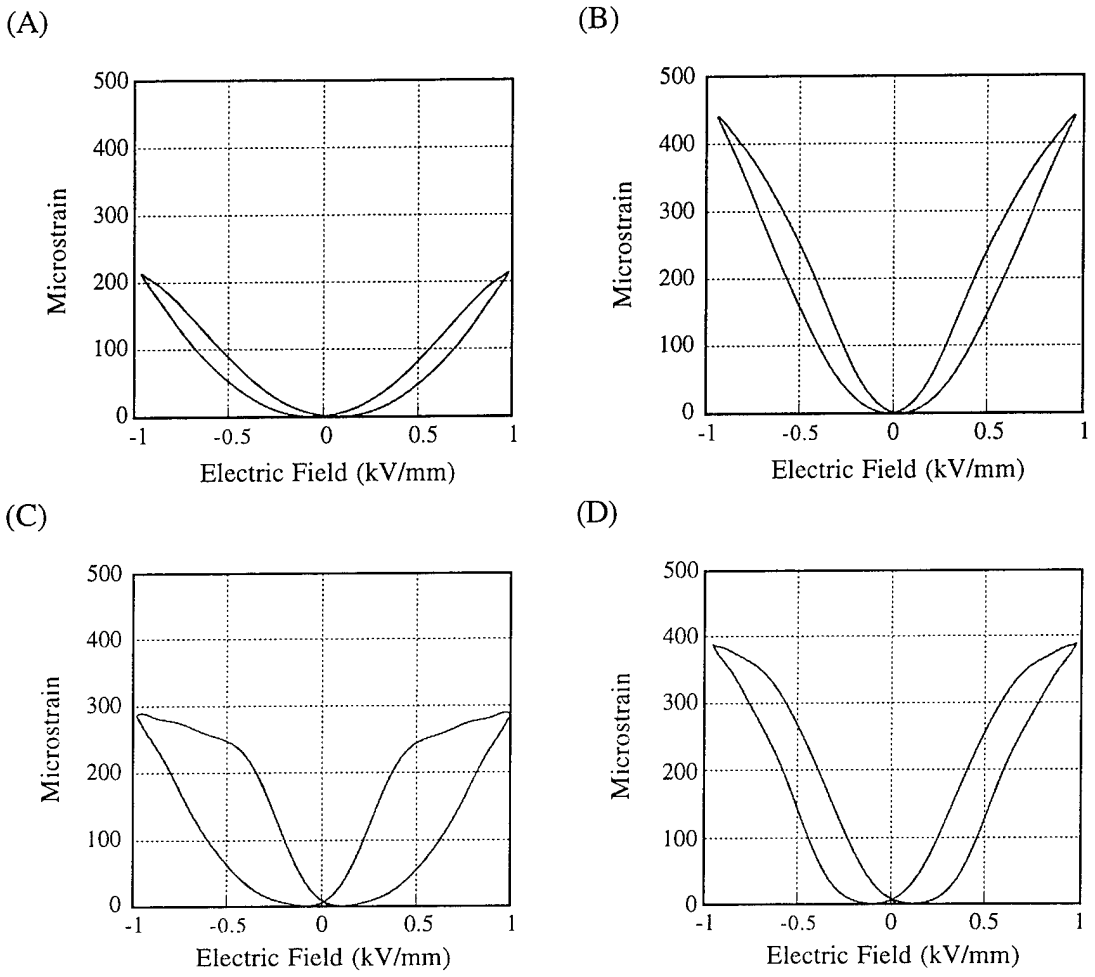

Figure 17. Plots of longitudinal strain vs. temperature for $0.96(0.91Pb(Mg_{1/3}Nb_{2/3})O_3 - 0.09PbTiO_3) - 0.04\ BaTiO_3$ samples with additives, sintered at 1200°C for 4 hr.: (A) PM-2, (B) PM-3, (C) PM-4 and (D) PM-5.

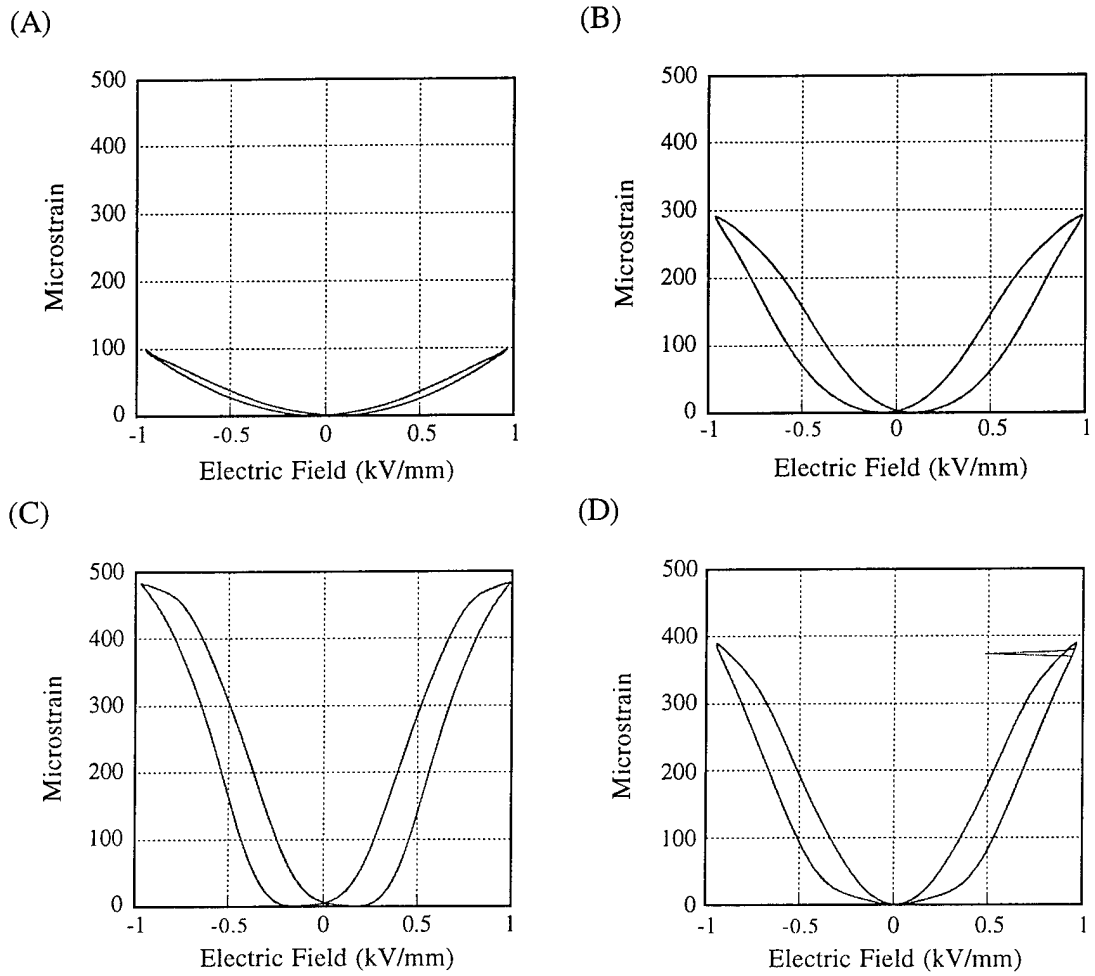

Figure 18. Plots of longitudinal strain vs. temperature for $0.96(0.91Pb(Mg_{1/3}Nb_{2/3})O_3 - 0.09PbTiO_3) - 0.04 BaTiO_3$ samples with additives, sintered at 1200°C for 4 h: (A) PM-6, (B) PM-7, (C) PM-8 and (D) PM-9.

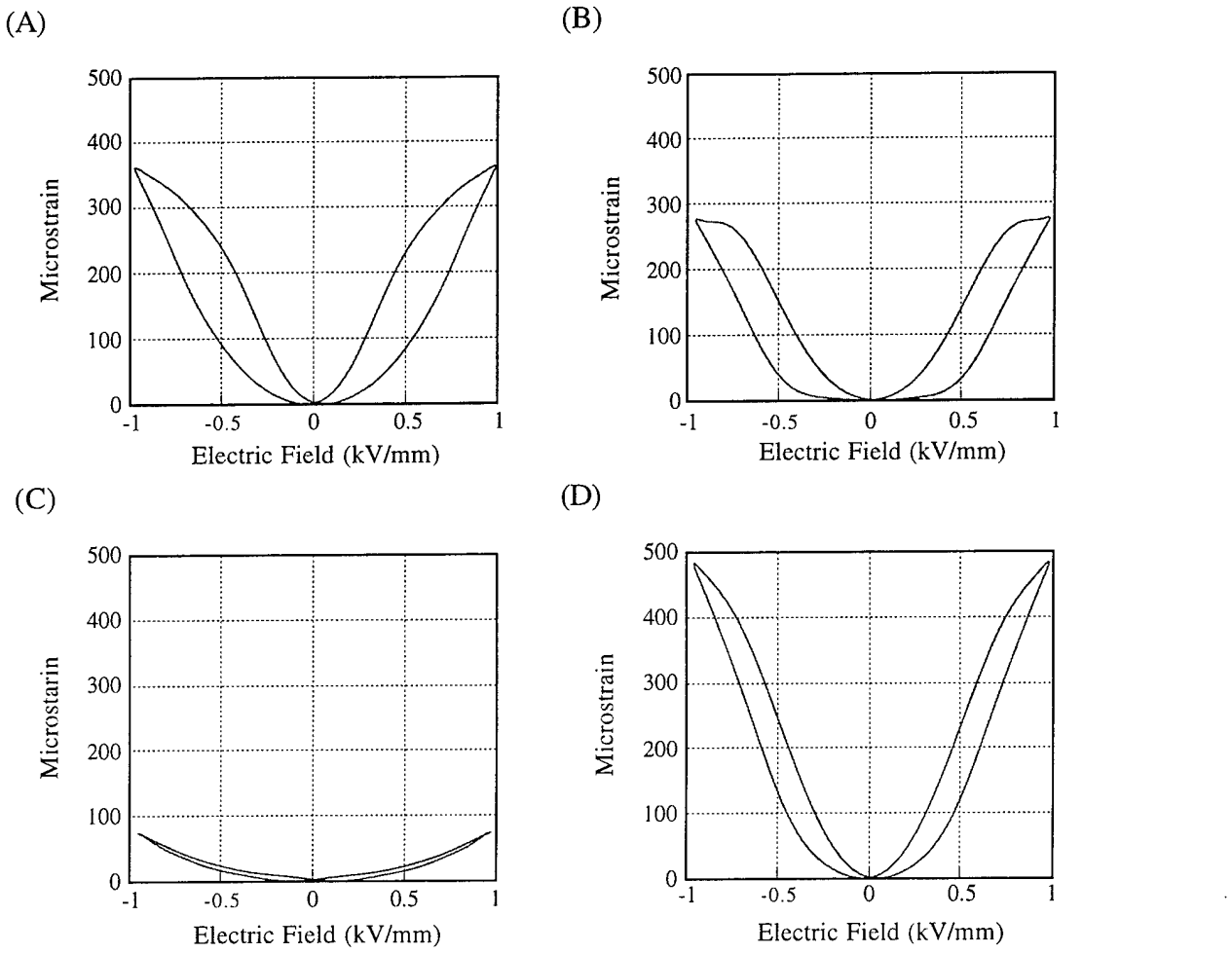

Figure 19. Plots of longitudinal strain vs. temperature for $0.96(0.91Pb(Mg_{1/3}Nb_{2/3})O_3 - 0.09PbTiO_3) - 0.04 BaTiO_3$ samples with additives, sintered at 1200°C for 4 hr.: (A) PM-10, (B) PM-11, (C) PM-12 and (D) PM-13.

5.4 Summary

Overall, a sol-gel method has been used to modify a base composition of a PMN material for electromechanical uses. The dielectric and electromechanical data obtained support the original hypothesis that modification by sol-gel is *different* than a conventional modification of composition. Although the exact mechanism is not understood, some modifications resulted in unexpectedly large changes in: T of k'_{max} , k'_{max} , and induced strain. Although understanding of this effect(s) might improve the performance of PMN's, the strain effect is most immediately important.

Specifically, PM-8 shows a doubling of the achievable strain at 1 kV/mm without increasing the polarization saturation. This translates into a **doubling** of the apparent electrostrictive Q constant. Although this is likely accompanied by some other, as yet undocumented deleterious changes in the

material, it is a very important result. The microstructure and density are good, the properties are outstanding, the mechanism and its optimization need examination.

5.5 References

1. L. E. Cross, Ferroelectrics, **76**, 241 (1987).
2. K. Uchino, Am. Ceram. Soc. Bull., **65**, 647 (1986).
3. H. Kanai, O. Furukawa, S. Nakamura and Y. Yamashita, J. Am. Ceram. Soc., **76**, 454 (1993).
4. S. M. Pilgrim, M. Massuda, J. D. Prodey and A. P. Ritter, J. Am. Ceram. Soc., **75**, 1964 (1992).
5. S. M. Pilgrim, M. Massuda and A. E. Sutherland, J. Am. Ceram. Soc., **75**, 1970 (1992).
6. Y. S. Cho and V. R. W. Amarakoon, J. Am. Ceram. Soc., **79**, 2755 (1996).
7. H. M. Giesche
8. B. C. LaCourse and V. R. W. Amarakoon, J. Am. Ceram. Soc. **78**, 3352 (1995).
9. H. M. Jang, J. H. Moon and C. W. Jang, J. Am. Ceram. Soc. **75**, 3369 (1992).
10. F. A. Selmi and V. R. W. Amarakoon, J. Am. Ceram. Soc. **71**, 934 (1988).

6. NOVEL APPROACHES TO TRANSDUCTION UTILIZING HIGH ENERGY PMN

6.1 Project Objective

Overall, the present program aims to develop a novel broadband 2-transducer set to produce high acoustic power across a bandwidth 1 - 6 kHz -- performance that currently requires at least 3 transducer types having different center frequencies. The overall objective of the transducer effort in the Phase I part of this program has been to develop implementable designs that best meet this goal. Included in this design objective are requirements that the transducers and the arrays into which they are configured have a broad band, be lightweight, possess high power densities and offer the driving electronics an efficient, low volt amp driving load. The units should also be depth capable to at least 600' and be deployable in a towed system. In order to meet these requirements the transducer design must at a minimum have:

- fractional bandwidth ($\Delta f/f_0$) > 84% (Q_m < 1.19)
- FOM > 200 W/kg/kHz

Complementing the transducer effort are a number of items dependent upon transducer design that have system implications which need to be considered. For littoral waters, a variable depth towed or airborne deployable system is desirable and the high-power-density transducers and arrays bring the challenge of minimizing cable size and the system electronics without compromising the acoustic performance. The bias voltage requirement of the high-power-density PMN places extra stress on the cable design and a specific objective added in the middle of the Phase-I program was to mitigate this problem. The approach to this part of the effort included a combination of electronic and transducer modifications to best accommodate the system considerations.

6.2 Work Performed

The principal focus of this Phase-I program was a modeling and design effort, taking the material properties of the PMN developed by Lockheed Martin and matching them to transducer types which will meet the broadband transduction goal. The materials work, described in Section 5 of this report has shown promising results in the development of higher strain, higher-coupling PMN but those data were not available in time for this study. It is our intention to include these material properties in the study in Phase II. The Active Signal modeling and transducer development team built on its inventory of model and transducer designs to first verify the models and designs and then explore enhancements of existing designs as well as investigate some new designs which would be particularly suitable for this application. The effort was a progressive one which proceeded along the steps:

1) Use existing experience to downselect from various candidate designs for this application

2) Verify the models for those designs

3) Using the same verified models, explore other candidate designs

4) Downselect to some optimum design which could be furthered during the Option component of the phase I program and be completed during the Phase II part of the program.

In parallel with the transducer design effort, we performed some exploratory studies on circuits which would allow the system complexity which generally goes hand in hand with PMN transducer technology to be simplified, making this technology more adaptable to platforms and systems hosting high-power, broadband arrays.

6.3 Candidate Transducer Designs

During the course of the work performed by the present Active Signal team while it was part of Martin Marietta and then Lockheed Martin, extensive modeling of various candidates was performed to determine an optimum candidate transducer type for the, then proposed, Lightweight Broadband Variable Depth Sonar (LBVDS) system -- now an ongoing Navy program. The result was an aluminum shell flextensional design with the advantages of being a proven design type, having an inherent mechanical transformer in the flexural design, having a record of good depth performance and high efficiency and being suitable for use in arrays with their potential array interaction considerations. We also built two of these arrays using PMN and their performance matched expectations. This design was, therefore, considered to be the baseline for this program.

The baseline design was however not optimized for bandwidth -- indeed power density and being a proven design with conventional ceramic drivers had been given a much higher ranking in the decision process. Having transducers not optimized for bandwidth in a broadband array leads to problems relating to the need for too many channels to achieve the bandwidth -- e.g., complexity of the driving electronics, especially in the area of biasing electronics and heavy cabling. It is on the basis of experience with this system that we have pursued the system enhancements which we believe are possible, while retaining the gains achieved through the development of PMN.

In this Phase-I program we set out to optimize a transducer design for bandwidth and produce designs tailored for PMN rather than use it as a drop-in to a conventional ceramic transducer design. The options we explored included aluminum flextensional transducers as the baseline,

graphite-epoxy (GrEp) flextensional units as a variant on this design, a flexural disk design, a mechanical amplifier design (i.e. moment bender with different amplification schemes), a slotted cylinder, a Tonpilz, a bender bar driving a flextensional shell, and a hybrid Class IV/Class VII, flextensional design. The design options under consideration and progress with them are listed in Table 1. Several of the designs eliminate the need for the large blocking capacitor as will be discussed later in this report and this is highlighted in the bias requirement column.

Table 4. Status of modeling studies of transducer designs.

Design	Bias Requirement	Status
1. Graphite flextensional	Requires full circuit	Complete
1a. Bender bar in graphite shell	Block cap. eliminated	Complete
2. Flexural disk	Block cap. eliminated	Complete
3. Moment bender	Requires full circuit	Complete
3a. Moment bender + mech amp	Block cap. eliminated	In progress
4. Slotted cylinder	Requires full circuit	Complete
5. Hybrid unit	Block cap. eliminated	Complete
6. Tonpilz	Requires full circuit	In progress

In this report we have taken our best knowledge of the design options, whether or not the analysis/optimization was complete, and attempted to cover the frequency range 1 - 6 kHz with two transducers of each option. At this point the GrEp flextensional and moment bender designs appear to be the most promising for the application based on bandwidth and power density (figure of merit). It must be noted, however, that several of the designs that eliminate the blocking capacitor are still works in progress. Since this can significantly lower ship impact by reducing the voltage and/or current on the cable, and hence reducing cable and winch size, we will continue to work on these innovative designs.

6.4 Broadband Design Results

In the actual modeling we conducted parametric analyses on transducer designs to optimize bandwidth and power density and then attempted to produce point designs for each option that cover the frequency range 1 - 6 kHz with just 2 transducers. The significant considerations in the design iterations were:

1) Emphasize designs which allow for the highest concentration of PMN in a compact transducer with a broad bandwidth.
2) In the use of models, begin with baseline models which match measured data on transducers which the staff of Active Signal have built while working for Martin Marietta so that our comparisons will have a realistic reference.
3) Explore some designs which allow for self-biasing capability of the transducers.

The criteria for selection of the best transducer design from all of the options are:

1) Highest fractional bandwidth for transducers in the 1 - 6 kHz range
2) Highest power density

3) Compact size compared to the center frequency wavelength (λ) such that the transducer can be used in a steerable array, which can readily be placed in a pressure vessel, if necessary, to avoid cavitation
4) Capability of operation at depths of ~600'
5) Ease of fabrication and robustness

Using these guidelines, we modeled several approaches to systems which utilize PMN drivers. The PMN properties used are those of the so-called 3rd-Gen material, which are now achievable, and so should be minimum values when compared to the PMN which is being developed under this program and which is described elsewhere in this report. All models are ones which we have developed and have proven against measured data or are NUWC models, such as FlexT5.6 which have proven reliable predictors of performance. We began with approaches which were conventional and then extended the study to include designs that could allow for self-biasing units to be built with no sacrifice to performance.

From simple algebraic considerations the two transducers covering the 1 - 6 kHz band should have relative bandwidths >84% and center frequencies (f_0) ~1.7 and 4.2 kHz. In creating these designs the sizes were estimated to correspond to the desired values of f_0 and the design was adjusted to maximize bandwidth based on our parametric studies for those options that had been completed or from known practice for those that had not been completed. Note that the designs were not adjusted to better match the desired frequencies after modeling. The designs were modeled and the center frequency and bandwidths (Δf) are calculated from the modeled SL vs frequency -- the bandwidths taken from the -3 dB power points on either side of f_0. The masses (m) of the transducers were estimated from the design dimensions and known densities of the materials. The power densities of the transducers were compared using the Navy's figure of merit (FOM - see Section 1). The methods used to arrive at the elements of the FOM were based largely on known transducer design parameters. Where we had to extrapolate the results of a known design to another frequency range of the same design, as in the case of the moment bender, we used the same principles of extrapolation so that the relative values should be valid even if some of the absolute numbers are not.

The respective performances of the point designs are summarized in Table 5 below and comments where appropriate are listed at the conclusion of the Table.

Table 5. Comparison of Various Transducer Designs for Frequency Range 1 - 6 kHz (Lo + Hi)

Transducer Type	f_0 (Hz)	$\Delta f / f_0$	SL @ f_0 (dB//μPa@m)	Efficiencies[1] max	Efficiencies[1] min	FOM (W/kg/kHz)
Lo Range Class IV GRP	1475	82%	208	60%	36%	432
Lo Range, Class IV Alum	1500	55%	209	63%	41%	305
Hi Range, Class IV GRP	3200	88%	201	58%	30%	308
Hi Range, Class IV Alum	3300	56%	201	60%	37%	228
Lo Range, Class VII GRP	1475	98%	207	53%	27%	349
Lo Range, Class VII Alum	1600	88%	206	49%	25%	251
Hi Range, Class VII GRP	3300	103%	199	53%	25%	350
Hi Range, Class VII Alum	3650	85%	199	48%	24%	250
Hi Range, Flex Disc	4000	18%	206	-[2]	-[2]	-[2]
Lo Range, Tonpilz PMN	1300	61%	210	47%	43%	357[3]
Hi Range, Tonpilz PMN	3200	108%	206	47%	43%	415[3]
Hi Range Al Mom. Bender	4200	55%	200	60%	35%	79
Hi Range GRP Moment Bender	4450	58%	204	64%	41%	224
Lo Range Al Mom. Bender	2150	86%	204	54%	10%	81
Lo Range GRP Moment Bender	2275	88%	208	61%	13%	200
Lo Range Ring Shell	1200	23%	214	81%	68%	203
Lo Range Split Cylinder	1734	111%	203	99%	-	672[4]
Hi Range Split Cylinder	4247	71%	200	99%	-	874[4]

1) When compared to known measured data, these numbers appear quite conservative. For instance, the modeled efficiency of a graphite flextensional transducer shown in the Table is 60% and our typical measured data shows that the units are 80% efficient at resonance and this takes into consideration directivity. Units with such high bandwidths as those in the Table have not previously been fabricated and so we do not have a direct comparison but we have been conservative in selection of material properties and so we believe the efficiencies listed in the Table are for the most part lower than are expected in practice.
2) The flexural disk estimates were based on hand calculations. Our acoustic modeler, Phil Kuhn, believes that because of the small mass of ceramic compared to the structure mass, the FOM will be low in all cases.
3) These numbers appear to be attractively high. However, they are based on assumptions of a transducer build from a set of unrealistic parameters as shown in the outline drawing which do not take into consideration either any depth compensation, accommodation for flexural resonances or extraordinary mechanical stress multipliers on the stacks. With no mechanical advantage in the design, we do not believe this to be a reasonable candidate.
4) Again, an attractive design just looking at the FOM figures. However, in the case of the Low Range PMN unit, the length is 49" (1.4λ) and for the high range, the length is 14" (1.0λ). This dimension was based on the requirement for a low Q device in this frequency range. This may also explain why the FOM and efficiency is high. The program takes into consideration horizontal directivity, but not vertical.

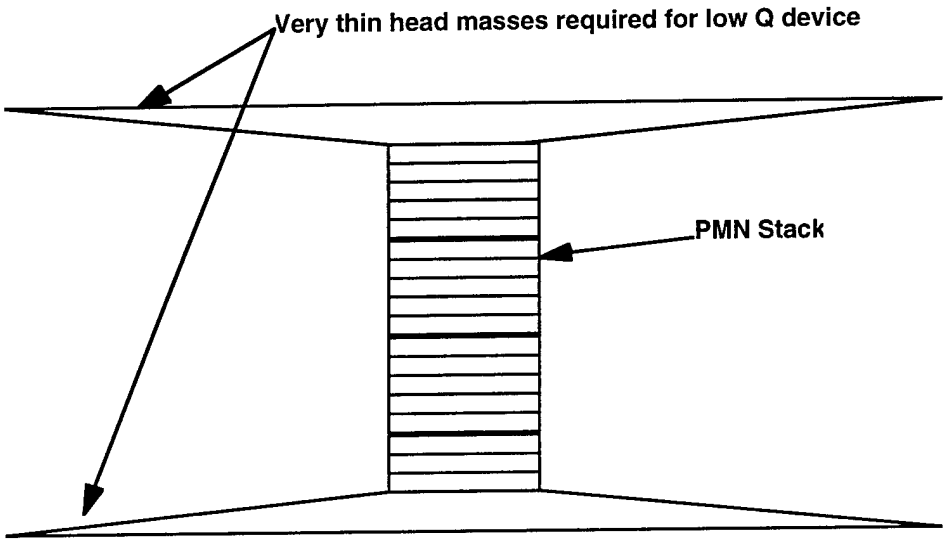

Figure 20. Outline drawing of Tonpilz transducer compared with a conventional flextensional unit showing both comparative size and area multiplier which make the design unworkable.

Table 5 reveals some not surprising but interesting points. First, the use of PMN in these designs yields very high FOM's. When we compared PMN to PZT as a driver for the split cylinder, for instance, PMN did yield a FOM approximately 10 times higher than PZT as well it should. Second, in all cases, the graphite composite design had a higher FOM than aluminum. We have found this to be true of PZT units we have built for communications transducers and did not expect that the results should change with either PMN as a driver or in designs which also used some flexural principal, such as the moment bender.

6.5 Confidence Level in Modeled Results

For a modeling and design exercise to have validity, some assurance of a correspondence between what is modeled and what is measured must exist. Thus, our first exercise was to verify that our models for a candidate transducer was matching measured data of transducers which were modeled. While the particular broadband designs in Table 5 have yet to be built and so no direct validation is possible, we were able to assess confidence levels based on evidence from similar transducer types.

The Navy's FlexT program is widely used and we had a high level of confidence in it for the baseline transducers. Since one of the important findings in this report is the improvement in bandwidth derived from using GrEp radiators it was especially important to validate a model for a transducer made from this material. A particularly suitable candidate for this exercise was a GrEp-shell PZT-driven Class IV flextensional transducer which we had built for a WQC-6 communications program directed by Jerry Schwell of NUWC and is shown in Figure 21[a]. This candidate transducer type matched our requirements of being a flextensional transducer and having a naturally broader band desired for this application due to the use of a graphite epoxy shell.

[a] John Sewell and Frank Hodges, *Advanced Designs of Communications Transducers*, presented at The Underwater Defense Technology Conference, Paris (1991).

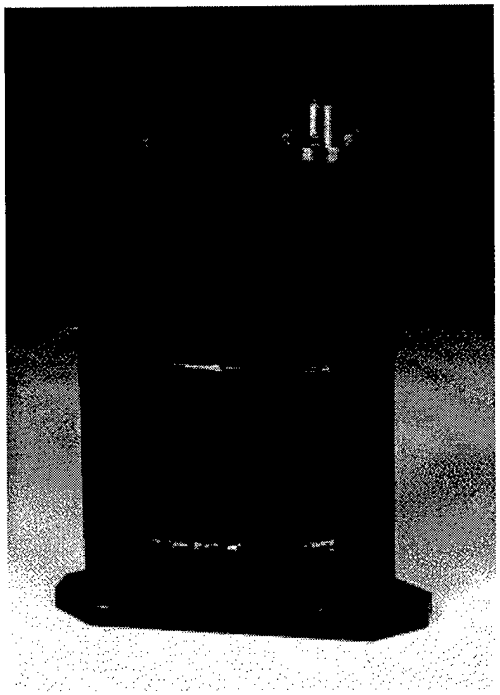

Figure 21. Graphite-epoxy flextensional transducer built by Active Signal Team for Jerry Schwell

The transducer selected had a resonance at approximately 2 kHz. In Figure 22 we show the measured data with the modeled prediction overlaid in a dashed line. Note that the model predicts a slightly lower TVR than the measurements show, especially at the high end or at 3 kHz. Around resonance and below the difference is just 1 - 2 dB but this increases to 4 dB at 3 kHz. The model used was FlexT5.6 and it predicts approximately a 1 dB directivity at 3 kHz whereas the measurements showed a 4 dB difference between the 0 and 90 degree axis measurements. The model correctly predicted the center frequency but underpredicted the bandwidth -- 28% vs a measured value of 38%. Overall, therefore, we believe that for the flextensional designs in Table 5 the predictions coming from the models indicate the minimum performance of the transducers as built. In other words we have a high level of confidence in those predictions.

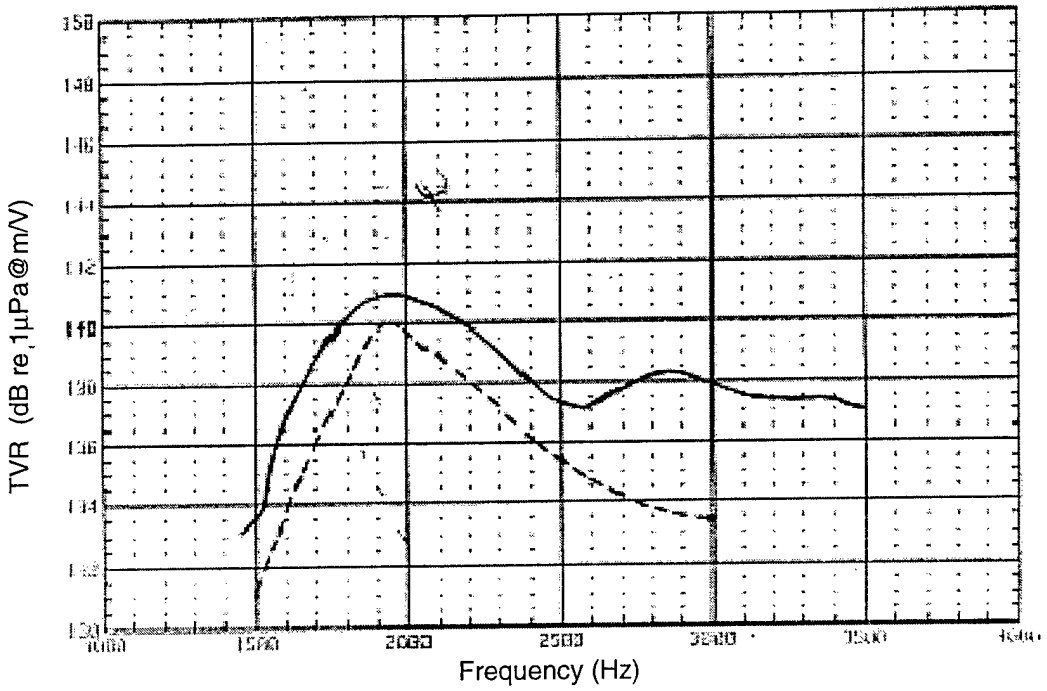

Figure 22. Modeled (dashed Line) vs measured results of 2 kHz graphite flextensional transducer.

The Tonpilz design in Table 5 clearly has problems with flexure etc. as discussed above so we did not spend more time validating the model -- although based on our experience with torpedo arrays with have a high level of confidence in it. The other design worthy of discussion is the moment bender. Active Signal has built several small versions of these for use as sensors and one as a pump. We have, however, never, built one for use as an acoustic projector but based on our experience with the units we have built the models, including the one we developed, tend to overpredict the deflection of the radiating disk and so we do not consider the predictions in Table 5 for this transducer class to be conservative. Nevertheless, this class still looks very promising based on the predictions in Table 5.

6.6 Downselect to an Optimum Design

At this point, we would probably select a GrEp flextensional transducer using our advanced PMN material as a new baseline transducer based on the 5 selection criteria and the data in Table 5. If we then added the requirement that there be a self biasing capability described in the next section, we would select from transducers having different acoustics vs. electrical phase relationships, and build a symmetrical hybrid transducer from them. Thus, we could select a transducer with a half-shell of Class IV flextensional design, and mate it with another half shell of a Class VII design in the place of the original Class IV second half shell. In this case, we would have two half shells with stacks driving out of phase to accommodate the self-biasing scheme, but with acoustic energy in phase. While this is a far more risky approach, it does combine designs with known capabilities, and can, at least theoretically, be built.

6.7 Parallel Self-Biasing Circuit Study

While PMN can reduce the size of a high-power array and its towbody by up to a factor of ten, it requires application of an external dc bias voltage which leads to very high voltages (>5 kV) on the tow cable which in turn makes the size of that cable and its winch significant in terms of ship impact. The largest contributor to the cable voltage is the bias voltage which is in the range of 18 V/mil (of plate thickness) and which now must go down the cable. This combined with the signal voltage amplified topside leads to the high-voltage stress on the cable -- over twice that of a conventional PZT system. In addition, the stacks are now driven in parallel which means that the conductors in the cable must be large enough to carry the total current for each unit which is also large due to the lower impedance of the high-power-density transducers. The high voltages and current combined stacks results in a cable which is the dominant weight in the system. The cable alone can weigh much more than the towbody and transducer array combined. In our study we set out to make the cable much lighter by a reduction of the voltage or current requirements and ideally both.

The following sketches show the current options for biasing and driving PMN transducers. The left side of the cable is the dry topside part of the circuit and the right side is the wet end. The options are described briefly and compared in the summary table. In the configurations shown the plate thickness is assumed to be 0.200" and the maximum drive is 10 V/mil with no tuning inductors. An equivalent, but much less powerful, PZT transducer would therefore require a peak voltage of 2.8 kV on the hot wire and its return would have approximately zero volts. No bias is required for PZT so its voltage derives entirely from the ac drive. It will be shown that Option 4 comes very close to meeting the PZT drive condition but because a push-pull circuit is used that Option imposes an equal but opposite phase voltage on the return wire.

Option 1: Current drive configuration

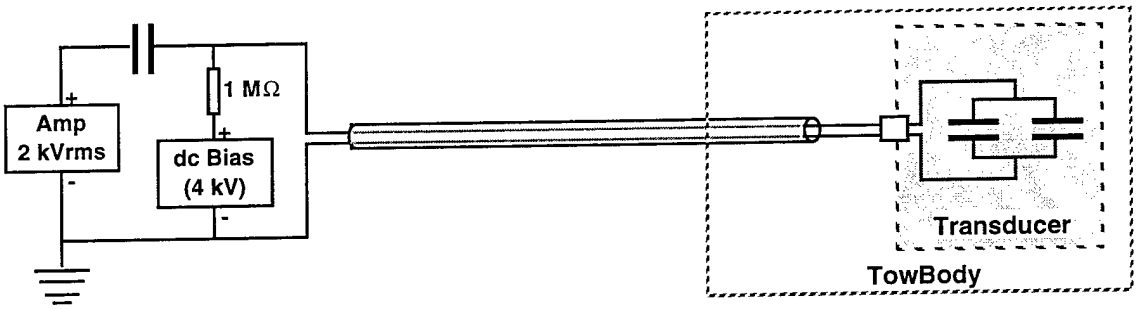

This is the configuration that has been used for most of the testing of PMN transducers done by Lockheed Martin and NUWC. The principle disadvantage is that the bias voltage and the peak drive voltage sum together on the hot lead to the transducer. This wire in the cable, therefore, must be able to withstand 6.8 kV ($4 + 2\sqrt{2}$). The return lead to ground on the other hand sees a relatively low voltage -- essentially zero. The principle advantage of this set up is that it has been tried and tested.

Option 2: Current drive configuration with bias on the return (low) side

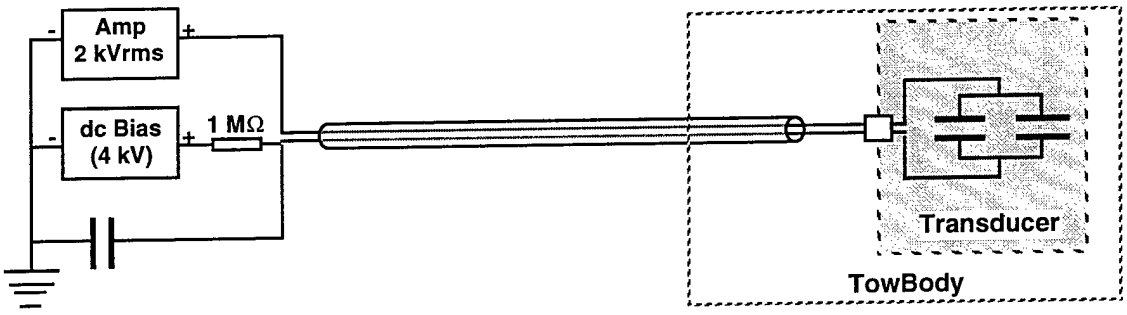

This option places the bias on the return side of the transducer thereby spreading the voltage load between the two leads in the cable. The peak voltage on the hot wire is now 2.8 kV and that on the return wire is 4 kV. Note that the peak voltage difference between the two wires is still 6.8 kV.

Option 3: Biasing in between the 2 stacks

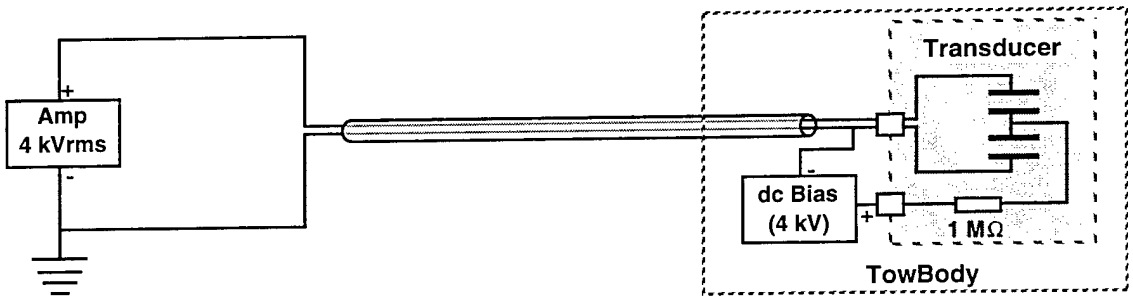

This option eliminates the large blocking capacitor(s) and so the bias supply can be moved down into the towbody. The bias supply will still need a 120-V prime power source but this wire is not shown for simplicity since a twisted pair of 120-V, low amperage leads will have minimal impact on cable size and cost. Note that just one bias supply is required for an array of like transducers but they must be electrically isolated from each other, e.g., with a high (1 MΩ) resistor. The 1-MΩ resistor is shown in the transducer but it could equally be housed elsewhere in the towbody. The peak voltage on the hot lead is now 5.6 kV and that on the return is similar to Option 1. The reason the peak voltage is not lower is that the stacks are connected in series and so the drive voltage had to be doubled. The principle disadvantage of this configuration is that the two stacks now operate out of phase and so a special transducer has to be designed.

Option 4: Biasing in between the 2 stacks and using a push-pull drive couple

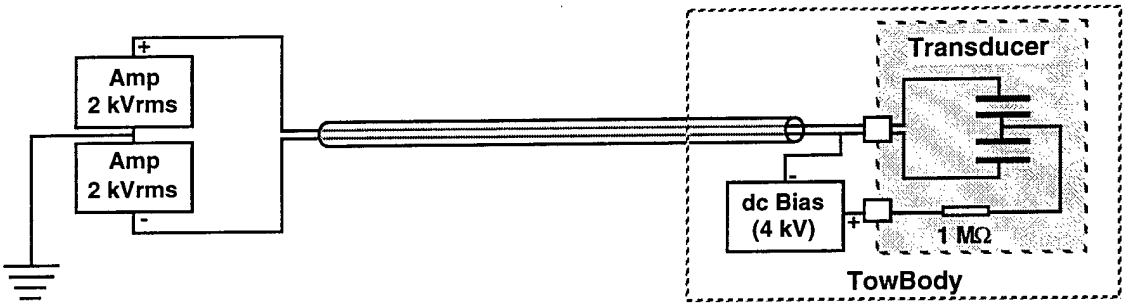

This option is similar to Option 3 but achieves the higher drive voltage with a push-pull amplifier configuration thereby spreading the voltage load between the two leads in the cable. The peak voltage on the hot wire is now 2.8 kV and that on the return wire is 2.8 kV. Note that the peak voltage difference between the two wires is still 5.6 kV.

Table 6. Summary of advantages and disadvantages of the drive-circuit options.

Option	Peak Voltage diff. (kV)		Advantages	Disadvantages
	Wire-Grnd	Hot-Retn		
1	6.8	6.8	• Simple circuit • Tried and tested • Return wire has little or no voltage on it	• Highest voltage stress on cable
2	4.0	6.8	• Evens out voltage stress on wires • Lower peak voltage to ground than Option 1	• Higher volt. stress on return wire
3	5.6	5.6	• Lower voltage stress on cable • dc component has been removed • Current in cable reduced by 50% • Return wire has little or no voltage on it	• Stacks run out of phase -- new transducer design required • Accommodation must be made for watertight bias supply in towbody
4	2.8	5.6	• Evens out voltage stress on wires • Lowest peak voltage to ground • Current in cable reduced by 50% • Most similar to PZT drive case	• Higher volt. stress on return wire • Stacks run out of phase -- new transducer design required • Accommodation must be made for watertight bias supply in towbody

In addition, we are exploring the possibility of a self biasing circuit which is shown in Figure 23. In this case the bias voltage is taken as a rectified tap from the ac drive signal. This would be more useful for the case where there is just one larger (lower frequency) transducer instead of an array and it uses a tuning inductor. We should emphasize that we are exploring several options for this and that none of the electrical circuits has been modeled with a transducer. At this stage our objective was to demonstrate that the bias voltage could be removed from the cable.

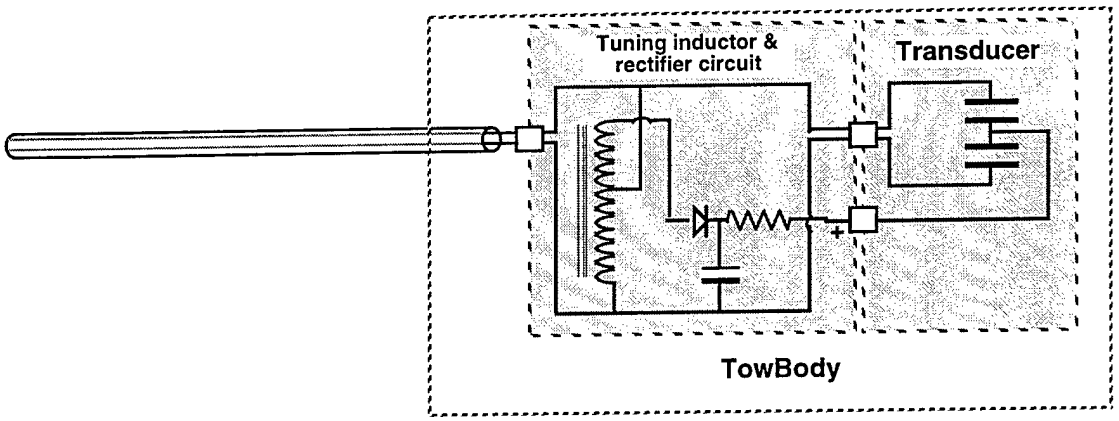

Figure 23. Self Biasing circuit for PMN transducers.

The net result of this approach is a reduction of approximately 60% in total voltage, a reduction of 50% in the current carrying requirements of the cable, the elimination of the blocking capacitor, and a considerable reduction in cable size and weight for the same array. These system gains make pursuing the transducer designs that allow for out-of-phase stacks very attractive. This effort will extend into Phase II of the program but the preliminary indicators as shown in this example are that simplifications to the system are possible using creative designs for the system electronics.

6.8 Estimate of Technical Feasibility

Technical feasibility of the areas explored under the transducer effort of the Phase I STTR was a criterion for our investigation of both transducer and biasing circuit options. In all cases the transducers and/or circuits under consideration had to be feasible, that is able to be developed within reasonable cost and schedule constraints or we did not continue the investigation. With that said, some distinctions within the groups are in order so that the outputs of the study can be assessed as we see them.

With respect to the technology insertion of a GrEp shell transducer using PMN in a current towed system in such a way as to broaden the band, while still being able to contain the array(s) in a pressure vessel, if necessary to avoid cavitation, this is certainly feasible. We have demonstrated the capability of GrEp shell technology within this band and have done it successfully as the endorsement letter of Jerry Schwell[b] attests. The littoral water depth requirements are certainly less than those in which the current units, built for blue water, now operate. We see no risk in creep, as with some composites such as fiberglass, since GrEp has a very low creep rate if it can be detected at all. This information is based on both actual performance of units already built as well as extensive modeling done by DuPont as part of the GrEp shell development effort for Martin Marietta.

With respect to an extrapolation to other types of units such as the Class VII shell made of GrEp, the feasibility of such a unit needs to be explored, but there appears to be no inherent inconsistency in the design or its implementation. We propose to discuss this with ARC as well as our other supplier as part of an implementation effort in Phase II.

---

[b] Jerome A. Schwell, Memorandum: *Flextensional Transducer Experience*, December 12, 1997

In the last part of the investigation in the transducer area, the self-biasing circuits, again we see no problem with implementation assuming that the transducers can be built so that half of the units operate out of phase with the other. Beyond this higher risk approach, the other options discussed such as simply putting the bias supply in the towbody, are lower risk, and we see no risk of their being unfeasible, especially given the design capability and experience of our team.

In summary, we believe the designs discussed in this final report are all feasible, except where pointed out. In the case of our preferred options, we readily agree that they have not yet been tried and therein lies the challenge. But as a team we have been highly successful and developing the as yet untried into working systems and are as anxious to demonstrate here again this capability in the succeeding phase of this program.